

*Microsolvation in $V^+(H_2O)_n$ Clusters Studied
with Selected-Ion Infrared Spectroscopy*

P. D. Carnegie,¹ J. H. Marks,¹ A. D. Brathwaite,² T. B. Ward,¹ M. A. Duncan^{1*}

¹Department of Chemistry, University of Georgia, Athens, GA 30602, U.S.A.

²Department of Chemistry, Emory University, Atlanta, GA 30322, U.S.A.

*Email: maduncan@uga.edu

Abstract

Gas phase ion-molecule clusters of the form $V^+(H_2O)_n$ ($n = 1-30$) are produced by laser vaporization in a supersonic expansion. These ions are analyzed and mass-selected with a time-of-flight mass spectrometer and investigated with infrared laser photodissociation spectroscopy. The small clusters ($n \leq 7$) are studied with argon tagging, while the larger clusters are studied via the elimination of water molecules. The vibrational spectra for the small clusters include only free O-H stretching vibrations, while larger clusters exhibit red-shifted hydrogen bonding vibrations. The spectral patterns reveal that the coordination around V^+ ions is completed with four water molecules. A symmetric square-planar structure forms for the $n = 4$ ion, and this becomes the core ion in larger structures. Clusters up to $n = 8$ have mostly two-dimensional structures, but hydrogen bonding networks evolve to three-dimensional structures in larger clusters. The free O-H vibration of AAD (acceptor-acceptor-donor) coordinated surface molecules converges to a frequency near that of bulk water by the cluster size of $n = 30$. However, the splitting of this vibration for AAD- versus AD-coordinated molecules is still

different compared to other singly-charged or doubly-charged cation-water clusters. This indicates that cation identity and charge-site location in the cluster can produce discernable spectral differences for clusters in this size range.

I. Introduction

The solvation of metal cations by water underlies many important chemical systems, such as electrochemical reactions, acid-base chemistry, atmospheric aerosols, and the many aqueous biochemical processes that govern life itself.¹⁻⁴ The molecular details of cation-water interactions have been investigated with many studies of the mass spectrometry of gas phase ion-molecule complexes,⁵⁻²⁵ and with corresponding computational studies.²⁶⁻⁴³ Collision-induced dissociation measurements have determined cation-water binding energies, while computational studies have provided structures, relative energetics and predicted spectra for complexes with different numbers of water molecules and different charge states. Spectroscopic experiments in either the UV-visible or infrared regions have determined the structures and the coordination numbers of different metal ions interacting with water.⁴⁴⁻⁸⁶ In the present report, we use mass spectrometry and infrared photodissociation spectroscopy to investigate the solvation of singly charged vanadium ions by multiple water molecules.

The spectroscopy of hydrated metal ions has examined the solvation effect of water on the atomic transitions of metal ions and the polarization effect of metal ions on the structure and bonding in water molecules. Electronic spectroscopy of mass-selected ions examined the atomic transitions in transition metal cations and those of alkaline earth metal cations bound to one or more water molecules.⁴⁴⁻⁵⁸ Among this group, Brucat and coworkers reported the electronic spectra for $V^+(H_2O)$,⁴⁴ our group and those of Fuke and coworkers and Kleiber and coworkers investigated alkaline earth cation complexes with water,^{45-48,51-53} and the group of Kleiber and that of Metz studied other transition metal cation-water complexes.^{54,56-58} Unfortunately, these electronic spectra of cation-water complexes exhibit sharp vibrational structure only for those species containing a single water molecule. Apparently, predissociation in excited electronic states leads to broad, continuous spectra for multi-water complexes. Infrared spectroscopy has

been more successful in revealing the solvation of metal ions. Infrared measurements in the O–H stretching region have been described for several different metal ions for complexes containing enough water to form the first, and sometimes larger, solvation spheres.⁵⁹⁻⁸⁶ These spectra reveal the so-called free-OH vibrations for the small clusters, which are usually shifted to lower frequency than the vibrations in water itself because the charge transfer toward the metal ion removes bonding electron density from the water. In larger complexes, hydrogen-bonded O–H stretches are shifted even further to lower frequency when water molecules beyond the initial coordination sphere are present. Specific structures for solvation complexes have been identified by comparison of infrared band patterns to the predictions of theory. There are several examples of spectroscopic studies on multiply-charged cation-water complexes.^{55,68-71,74,75,78,79,81} Williams and coworkers have reported infrared spectra on several such systems for clusters in the size range extending up to 30–50 water molecules.^{68-71,78,79} The only other study of large singly-charged metal cation-water clusters is that of the $\text{Ni}^+(\text{H}_2\text{O})_n$ system.⁶⁵

Vanadium-water complexes have been the focus of several previous studies, including electronic spectroscopy and infrared spectroscopy.^{44,60,72,81,86} Our research group has documented the infrared patterns for the $\text{V}^+(\text{H}_2\text{O})$ complex using infrared photodissociation with different rare gas "tag" atoms attached.⁸⁶ Spectra with partially resolved rotational structure revealed evidence for ortho-para conversion on the water molecule catalyzed by the metal. We also reported the variation of water vibrations for singly vs doubly charged vanadium ions.⁸¹ Sasaki et al. used similar photodissociation methods to study $\text{V}^+(\text{H}_2\text{O})_n$ ions for $n = 3-8$ using tagging with nitrogen or the elimination of water molecules.⁷² Unfortunately, this latter study had broad bands because of the multiphoton excitation and/or warm thermal conditions of the ions. In this work we employ rare gas atom tagging to improve the signals for the smaller multi-

water complexes, and we extend the study to larger cluster sizes, revealing the effects of solvation in this system.

EXPERIMENTAL

Vanadium-water complexes of the form $V^+(H_2O)_nAr_m$ were produced in a laser vaporization/supersonic molecular beam cluster source.⁸⁷ A representative mass spectrum is presented in the Supporting Information as Figure S1. Specific ions were mass-analyzed and selected for photodissociation measurements in a reflectron time-of-flight mass spectrometer.^{88,89} Infrared excitation was accomplished with a Nd:YAG-pumped OPO/OPA laser system (LaserVision).⁹⁰ We used ion cooling and inert gas atom tagging strategies developed in many recent studies of ion spectroscopy.⁹¹⁻¹⁰⁶ The photofragment yield was recorded as a function of the infrared laser energy using a digital oscilloscope (LeCroy) to measure the infrared spectrum. Infrared spectra were compared to the band patterns predicted by theory to determine the structures and spin states of the complexes.

Computational studies were performed on these clusters at the DFT/B3LYP level using Gaussian09.¹⁰⁷ The Def2-TZVP basis set was used for vanadium and the 6-311+G(d,p) was used for hydrogen, oxygen and argon. Vibrations resulting from harmonic computations were scaled by a factor of 0.96 to account for anharmonicity,¹⁰⁸ except as noted. In the case of the $V^+(H_2O)Ar_2$ complex, anharmonic vibrational theory computations were performed using the VPT2 method.

RESULTS AND DISCUSSION

Figure 1 shows the spectra for the $V^+(H_2O)_n$ complexes for $n = 3,4,5,7$ measured by the elimination of water molecules. Smaller clusters do not dissociate efficiently by eliminating

water. Spectra of this kind were reported previously for some of these cluster sizes by Sasaki et al.⁷² As shown, the spectra contain broad noisy bands because of the low dissociation yields. According to computational results, the binding energy of water to these clusters is higher than the photon energy used for excitation. Therefore, dissociation can only occur if there is multiphoton absorption, or if these clusters are not cooled completely and have some residual internal energy. The spectra for the $n = 3$ and 4 complexes contain two bands each (3607/3685 and 3617/3699) assigned previously⁷² to the symmetric and asymmetric stretches of the water molecules. These bands are shifted to lower frequencies compared to the stretches of water itself (3657 and 3756 cm^{-1})¹⁰⁹ because of the polarization of the water by the metal ion, which removes electron density from the O–H bonds and thus lowers the frequencies. The relative intensities of these bands (i.e., near equal) contrasts markedly with the spectrum of water itself, where the asymmetric stretch is much more intense than the symmetric stretch.¹¹⁰ The enhancement of the symmetric stretch intensity is also attributed to a polarization effect from the metal ion. The $n = 5$ complex has bands in this same region, but new features further to the red (3352, 3511 cm^{-1}) in the region assigned to hydrogen bonding vibrations. Similar structure in this region is seen for the $n = 7$ complex. This first appearance of these hydrogen bonding bands for the $n = 5$ complex establishes that the coordination around the vanadium ion is complete with four water molecules. This can be compared to $\text{V}^+(\text{CO}_2)_n$ clusters, where the coordination is also four,¹¹¹ or to $\text{V}^+(\text{CO})_n$ complexes, where the coordination is six.^{112,113}

Because of the low signal levels from spectra measured under the conditions of Figure 1, and the possible detection bias toward warm clusters with unquenched internal energy, we measured spectra for the vanadium cation-water complexes in this same size region using argon tagging. Tagging allows the detection of spectra by single-photon dissociation, and guarantees that the clusters are cold. Figure 2 shows the spectra obtained for the $\text{V}^+(\text{H}_2\text{O})_n\text{Ar}$ species for n

= 1–7. Sasaki et al.⁷² reported corresponding spectra for the $n = 2–4$ species tagged with N_2 . Comparison of our argon-tag spectra to the N_2 -tag spectra of Sasaki et al. shows that our spectra have more multiplet structure for each cluster size and generally narrower linewidths (10–15 cm^{-1} here vs 30–40 cm^{-1} in ref. 72). Because supersonic cooling in different expansion gases and cluster sources may affect ion temperatures, and the different binding energies of nitrogen versus argon to these clusters may produce different structures and photodissociation efficiencies, it is not too surprising that the spectra produced in the two experiments might be different. The higher resolution for clusters up to $n = 7$ provides an opportunity to compare these spectra to the predictions of theory to investigate which structures might be present for each cluster size. As shown, each of these spectra have sharp features in the free-OH stretching region, and those for $n \geq 4$ have red-shifted bands in the hydrogen bonding region.

Figure 3 shows the spectrum of the mono-hydrated $V^+(H_2O)$ complex tagged with two argon atoms compared to the spectra predicted for this complex with theory. Two O–H stretch bands are detected at 3620 and 3691 cm^{-1} . The spectrum of this ion tagged with a single argon or neon atom produces partially resolved rotational structure, which has been analyzed and discussed extensively in previous work.^{60,86} The band patterns and partially resolved rotational structure were consistent with a C_{2v} metal-water structure. The two main bands shown here at 3620 and 3691 cm^{-1} are shifted to the red from the vibrations of water. As shown in the figure, the most stable structures for this ion consists of a C_{2v} cation-water unit with argons attached asymmetrically to the metal ion opposite the water. The quintet spin state (corresponding to the d^4 ground state configuration of V^+) is predicted to be the most stable electronic ground state for the ion. It has two O–H stretches matching the experimental bands. As shown, the corresponding triplet and singlet states have similar predicted spectra, making it impossible to

confirm the ground state from this data alone. There is additional uncertainty because DFT is known to have difficulties in determining the relative energies of spin states for transition metals.¹¹⁴⁻¹¹⁸ However, the rotational analysis and high level theory in our previous work demonstrated that this complex has the quintet ground state when it is tagged by a single argon or neon atom,⁸⁶ and therefore we conclude that the same is likely true when it is tagged with two argons, consistent with the energetics predicted here by DFT. The weak band at 3881 cm⁻¹ is not predicted by theory, and is therefore likely a combination band involving an argon stretch. Such combination bands have been seen in several previous studies of cation-water complexes tagged with argon.⁷³

Figure 4 shows a spectrum of the same V⁺(H₂O)Ar₂ ion extending into the near infrared region. Additional bands are detected at 5280, 7121 and 7150 cm⁻¹ in regions corresponding to the O–H stretch/OH₂ scissors bend combination and the O–H stretch overtones. As shown, anharmonic theory computations predict a $\nu_2 + \nu_3$ bend-stretch combination at 5208 cm⁻¹ in reasonable agreement with the experiment, and $\nu_1 + \nu_3$, $2\nu_1$ and $2\nu_3$ overtones at 7032, 7050 and 7165 cm⁻¹ in less agreement with the experimental pattern. Results of similar mixed theory-experiment agreement were obtained recently for near-IR spectroscopy of protonated water clusters.¹¹⁹ This is another example of the limitations of the VPT2 method for such systems. Because of the lower intensities of overtones and combinations, and the lower parent ion concentrations, we were not able to obtain near-IR spectra for larger clusters.

Figure 5 shows the spectrum for V⁺(H₂O)₂Ar compared to the spectra predicted by theory for different structural isomers of this ion. Because of the discussion above about spin states, and the computational data for different spin states provided in the Supporting Information, we focus here on quintet states with different binding arrangements for the two water molecules or different attachment sites for the argon. The experimental spectrum consists of five bands (3576,

3609, 3670, 3684, 3720 cm^{-1}), with the lowest energy four of these forming two doublets. For comparison, the nitrogen-tagged complexes studied by Sasaki et al. produced bands at 3614 and 3688 cm^{-1} .⁷² Isomer 2a, which has the two water molecules opposite each other and argon binding to an OH of one water, accounts for two doublets that match the spectrum. The two bands predicted for isomer 2b, which has the two waters opposite each other but the argon bound to the metal ion, fall in almost exactly the positions to overlap the 2a spectrum. Because the energies of isomers 2a and 2b are computed to be the same, we can expect that both are probably present. The highest energy band at 3720 cm^{-1} is not explained by either of these lower energy isomers, but the spectrum of isomer 2c has a band (3734 cm^{-1}) that could explain this higher energy feature. Isomer 2c is somewhat higher in energy, but it appears that a small amount of this structure may also be present. Therefore, already the complex with two waters and an argon seems to have at least three co-existing isomers.

Figure 6 shows the spectrum for the $n = 3$ complex compared to those predicted by theory for different low-lying isomers. Bands detected here at 3613, 3628, 3691, 3708 and 3758 cm^{-1} can be compared to the two broader bands at 3617 and 3693 cm^{-1} detected by Sasaki et al.⁷² or to the two features at 3607 and 3685 cm^{-1} measured here without tagging (Figure 1). Isomers 3a and 3b have virtually the same energy and differ only in the binding position of argon. Isomer 3b has a pair of doublets that matches the experimental spectrum reasonably well. This same pattern is also predicted for the tag-free ion (see Supporting Information). With the possible exception of the weak signal detected near 3758 cm^{-1} , the patterns predicted for isomer 3c do not appear to be present in the experimental spectrum. The weak signal at higher energy may be coming from a minor amount of the high frequency band in isomer 3c, or it may also be coming from a weak combination band. In any event, the three-coordinate water ion structure seems to explain the main structure in the spectrum.

Figure 7 shows the experimental spectrum for the $n = 4$ ion, compared to the patterns predicted for several of its possible isomers. The bands at 3504, 3626, and 3708 cm^{-1} can be compared to those detected by Sasaki et al. at 3620 and 3694 cm^{-1} ,⁷² or to the two bands at 3617 and 3699 cm^{-1} measured here without tagging (Figure 1.) Theory predicts a four-coordinate species with a near square-planar structure to be most stable. As seen for the $n = 3$ ion, bands are predicted near the positions of two O–H stretch features, but theory seems to over-emphasize the effects of multiplet structure introduced by different argon attachment sites. A weak band at low frequency (3504 cm^{-1}) can only be explained by hydrogen bonding, and a 3 + 1 coordinated structure with the external water in a double-acceptor configuration has a hydrogen bonding band in the correct position. This hydrogen bonding band is predicted to be rather intense, making it possible to see this vibration even if there is only a minor concentration of this species. In the tag-free spectroscopy (Figure 1), hydrogen bonding was not detected until the $n = 5$ cluster, suggesting that the $n = 4$ had only a four-coordinate structure. However, at the lower temperatures of the argon tagging experiment, a minor concentration of a 3 + 1 isomer is not unreasonable.

Figure 8 shows the experimental spectrum for the $n = 5$ ion, compared to the patterns predicted for several of its possible isomers. The experimental spectrum here is simpler than those for the smaller clusters, with only two main bands at 3517 and 3702 cm^{-1} . These occur in the free O–H stretching region and in the region of a hydrogen bonding vibration. For comparison, the free O–H feature for this ion measured without tagging occurs at 3699 cm^{-1} , in virtually the same position measured here. The tag-free ion has three bands in the hydrogen bonding region (3240, 3352, 3511 cm^{-1}), similar to the spectrum reported by Sasaki et al.,⁷² compared to the single feature here at 3517 cm^{-1} . As shown below and in other studies on these ions, the bands further to the red correspond to molecules with a single hydrogen bonding

connection, whereas the band near 3517 cm^{-1} corresponds to a more highly connected external water in a double-acceptor site. Theory shows that $4 + 1$ coordinated structures are most stable, confirming that the external water molecule is in such a double-acceptor configuration. The attachment of argon at different positions in isomers 5a and 5b seems to make little difference in their predicted spectra. Except for the doublet predicted but not resolved in the spectrum for the free O–H stretch, the predicted spectra match the experiment reasonably well. There seems to be no evidence for isomers 5c or 5d which have $4 + 1$ structures with the external water in a single-acceptor site.

It is understandable that vibrations for single-acceptor molecules would be present in the tag-free spectrum but not here, on the basis of both temperature effects and dissociation energies. Argon tagged clusters are generally colder than those produced without tagging because of the better cooling in argon expansions and the fact that argon will not attach efficiently to warm clusters. Tagged clusters therefore are more likely to access the lower energy structures. There is also likely a bias in the tag-free spectroscopy to detecting warmer clusters because these species have internal energy that can combine with the photon energy to achieve dissociation. Additionally, dissociation of the single-acceptor structures requires that only one hydrogen bond be broken, which can be achieved with a single infrared photon. Dissociation of the double-acceptor clusters requires the breaking of two hydrogen bonds and requires more energy. This effect would bias the tag-free spectroscopy toward the detection of single-acceptor clusters. With argon-tagging, the clusters are colder and argon binding energy is always far below the photon energy, so that any detection bias is eliminated. All these issues explain the difference between the spectra measured with versus without tagging.

The spectrum for the $V^+(H_2O)_6Ar$ ion is presented in Figure 9, where the band patterns are compared to those predicted by theory for possible isomeric structures. As shown, a

symmetric structure with a square-planar core ion and two second-sphere water molecules in opposite double-acceptor positions is predicted to be most stable. Isomers 6a and 6b have different argon attachment sites, but their spectra are virtually the same. Each has a pair of doublets whose positions match the main bands in the spectrum reasonably well, but their relative intensities are a little off. In the experimental doublet at 3504 and 3532 cm^{-1} the two peaks have almost equal intensities, whereas the bands here for isomers 6a, 6b (and 6c) have one intense peak and another much weaker one. It is not clear whether there is a problem with the computed intensities or that more than one isomer is present. Isomer 6c has the same structure as 6a and 6b, but with one of its external waters in a single-acceptor site. Its band in the 3500 cm^{-1} region is at higher frequency, and so a contribution from this might explain the experimental doublet. However, it also has a red-shifted hydrogen bonding bands near 3150 cm^{-1} that is not detected in the experiment. Isomer 6d has a structure and spectrum like that of 6c, but with a different argon attachment site. Isomer 6e is the only one having a band near 3590 cm^{-1} , which could explain the feature here in the experimental spectrum, but this is also unsatisfactory because the strong band predicted for this structure near 3400 cm^{-1} is not detected. Overall, it appears that structures like isomers 6a and 6b must be present, but it is difficult to explain the feature at 3592 cm^{-1} . The spectrum of the $n = 7$ cluster (see Supporting Information) is also difficult to assign.

We were unable to obtain efficient tagging for clusters larger than the $n = 7$ species, but found that clusters in this larger size range dissociate efficiently by eliminating one or more water molecules. We therefore measured spectra for the larger species in this way. As discussed above, this may introduce some biases into the structures of clusters that can be detected.

Figures 10, 11 and 12 show the spectra measured for the clusters up to a size of $n = 30$. Figure 10 shows the spectra obtained for the $n = 8, 11,$ and 14 species, which illustrate an evolution in

the spectral patterns. The $n = 8$ species has a spectrum with a doublet ($3696/3725\text{ cm}^{-1}$) in the O–H stretching region, and a prominent band in the hydrogen bonding region at 3391 cm^{-1} . The O–H doublet was seen for smaller clusters (e.g., $n = 3, 4, 7$ in Figure 1), but the spacing is now smaller. This region for the $n = 11$ and 14 clusters has more of a single broad band here, with perhaps a shoulder on the high frequency side. The 3391 cm^{-1} band is in the region of hydrogen bonding O–H stretches for external water molecules in a single-acceptor binding site. It appears to be following the progression of similar features at 3352 and 3371 cm^{-1} for the $n = 5$ and 7 clusters (Figure 1). These bands are not found for the argon-tagged versions of these ions, as the external waters in those structures are mostly in double-acceptor sites, consistent with higher connectivity at lower temperatures. This kind of hydrogen bonding band is not found for the $n = 11$ and 14 clusters, nor is it seen for any of the larger systems in Figures 11 and 12. Instead, the hydrogen bonding region has progressively less structure for the $n = 11$ and 14 clusters, and eventually takes on a smooth, structureless profile in the larger clusters.

These changes in the vibrational band patterns seem to be associated with a change in the clusters from two-dimensional (2D) to three-dimensional (3D) structures. The preference for 2D structures was already demonstrated in Figures 6–9, where the square-planar motif emerges for the $n = 4$ cluster, and then $n = 5$ and 6 species add external waters in the gaps between the inner-sphere molecules. To see how far this pattern goes, we did computational studies on randomly selected isomers of the $n = 8$ and $n = 10$ clusters. These computations are not likely to be complete, but they seem to illustrate structural tendencies. As shown in the Supporting Information, many of the $n = 8$ structures are planar or near-planar, whereas the $n = 10$ species have begun to form more 3D networks. These tendencies are consistent with the changes in the vibrational spectra. The 3391 cm^{-1} band for the $n = 8$ species is associated with external water with a single-acceptor connection, consistent with many of the structures found computationally.

As clusters begin to form 3D networks, fewer water molecules have such a single connection, and most are involved in both donor and acceptor sites. This leads to a broader hydrogen bonding absorption. In 3D configurations, the symmetric O–H stretch seen for the smaller clusters becomes inhibited and the only surviving kind of O–H stretch is that for the subset of molecules with one dangling/free OH, which then resembles the asymmetric stretch vibration in the smaller clusters. This explains the trend toward a single main vibrational band near 3700 cm^{-1} . As shown in Figures 11 and 12, the much larger clusters have likely converged to the 3D pattern, with a smooth hydrogen bonding region and a nearly-single band close to 3700 cm^{-1} for the free O–H stretch. It therefore seems that a transition from 2D to 3D clusters takes place in the $n = 8\text{--}10$ size range.

Figures 11 and 12 show the spectra measured for the larger clusters in the $n = 17\text{--}30$ size range. These all have a smooth, nearly featureless hydrogen-bonding signal in the $3400\text{--}3650\text{ cm}^{-1}$ range, and what appears to be mostly a single broad resonance near 3700 cm^{-1} corresponding to a free O–H stretch. These general features have been seen previously for other large cation-water clusters, including $\text{H}^+(\text{H}_2\text{O})_n$ protonated water,¹²⁰⁻¹²³ alkaline-earth $\text{M}^{2+}(\text{H}_2\text{O})_n$,^{69-71,78,79} and $\text{Ni}^+(\text{H}_2\text{O})_n$ species.⁶⁵ A trace of a dip near 3580 cm^{-1} occurs in the hydrogen bonding region, which is most noticeable in Figure 11. This has also been seen previously for other cation-water clusters. This suggests that the hydrogen bonding region for these clusters is inhomogeneously broadened, containing contributions from several partially overlapping hydrogen bonding resonances, and the dip represents a gap in this pattern.

It can be seen in Figures 11 and 12 that the broad free O–H band near 3700 cm^{-1} actually has some structure. Each of these bands has a shoulder on the high energy side spaced above the center of the main peak by about $18\text{--}20\text{ cm}^{-1}$. This doublet structure has been seen and discussed

before for several systems of large cation-water clusters.^{65,69-71, 78,79,120-123} It is associated with the free O–H stretches of two kinds of water molecules in the hydrogen bonding network. Fully coordinated water has two acceptor and two donor hydrogen bonds, leaving no free OH to contribute any absorption at this frequency. Water molecules having a single free OH can have either three (one donor, two acceptor; AAD) or two (one of each; AD) hydrogen bonding connections. These different coordinations have been shown to have a small, but non-negligible effect on the frequency of the free O–H stretch. Three-coordinate molecules are most common in a cold cluster, and contribute the intensity of the AAD band at lower frequency, whereas the two-coordinate molecules occur less frequently and give rise to the high frequency AD shoulder. The spacing between these two bands has been shown to vary with the identity of the cation in the cluster and with the size of the cluster.^{65,69-71, 78,79,120-123}

In the present system, the main band shows only a slight size dependence, occurring at 3705–3708 cm⁻¹ for clusters in the n = 17–30 size range. This can be compared to the free O–H stretch seen at 3700–3705 cm⁻¹ for water surfaces, measured with sum-frequency generation techniques.¹²⁴⁻¹²⁶ Apparently, in this respect, the surface O–H vibrations in the clusters in the 17–30 molecule size range are already essentially converged to the bulk behavior. The spacings between the two kinds of free O–H bands is quite large in the smallest clusters, in the range of 20–22 cm⁻¹ for the clusters in the n = 10 size range, and then as small as 17–19 cm⁻¹ in the larger clusters. Figure 13 shows a plot of the free O–H band spacing versus cluster size for the present vanadium cation clusters compared to those of protonated water clusters and nickel cation clusters studied previously in our group. As shown, all three systems have a lower spacing beginning near the cluster size of n = 10, consistent with the formation of three-dimensional structures discussed earlier. In the size range of n = 10–30, there is considerable scatter, but the

spacings for the metal ion systems are in the range of 17–22 cm^{-1} . The vanadium spacings are generally smaller than those of the nickel species. However, the protonated water clusters have systematically larger spacings of $>20 \text{ cm}^{-1}$. This is a small, but reproducible effect. Protonated water clusters in this size range are believed to have a hydronium ion in the wall of clathrate-like cage structures, whereas metal-containing clusters should have the cation more centrally located in a hydrogen-bonding network. In both kinds of systems, the free O–H vibrations carrying the information are located on the external surface of the cluster, separated from the charge carrier by 1–2 water molecules. Apparently, charge induction effects running through the hydrogen bonding network are significant enough so that surface water molecules not only feel a slightly different electronic environment for AAD vs AD coordination, but they also sense the identity and location of the charge in the cluster. Similar observations and conclusions have been reached by other studies of large cation-water clusters.^{65,69-71,78,79} The splitting is even larger ($\geq 25 \text{ cm}^{-1}$) for water clusters with doubly and triply charged metal ions than it is for the singly-charged species shown in Figure 13.^{69-71,78,79}

CONCLUSIONS

We have reported here a study of the solvation processes in singly-charged $\text{V}^+(\text{H}_2\text{O})_n$ clusters. Infrared photodissociation spectroscopy of mass-selected ions, supplemented by density functional theory calculations, monitors the kind of infrared oscillators present in these systems and how they evolve with cluster size. In the smallest clusters, water molecules are coordinated directly to the metal cation and the free OH stretches are shifted to lower frequencies because of the resulting polarization of bonding molecular orbitals on water. Beginning at the cluster size of $n = 4$, there is evidence for hydrogen bonding, and this grows and becomes more important in the larger clusters. In the larger clusters, there is a broad region of hydrogen-

bonding signal and a prominent free O–H stretching band. Because of the formation of the hydrogen-bonding network, the symmetric stretching mode seen in the free OH region loses intensity in the cluster size range of $n = 6–8$. By $n = 10$, the asymmetric stretch resonance becomes the signature of those water molecules with one free OH remaining. This "surface" OH stretch is already converged to essentially the frequency value of bulk water in clusters in the $n = 20–30$ size range. The free OH resonance splits into a doublet caused by the different inductive forces present for two-coordinate (AD) versus three-coordinate (AAD) water molecules. The doublet spacing varies with cluster size, and can be compared to values seen previously for other cation-water clusters. The spacings here are smaller than those seen for doubly-charged metal cation-water clusters, somewhat smaller than values seen for protonated water clusters, and comparable to values seen for singly-charged $\text{Ni}^+(\text{H}_2\text{O})_n$ clusters. This variation in surface spectral features for different cations in cluster sizes up to 30 molecules of water, indicates that the inductive forces in hydrogen bonding networks reach out into the second sphere molecules, and perhaps beyond.

Acknowledgments

We gratefully acknowledge the generous support for this work from the National Science Foundation through grant no. CHE-1764111 and the U. S. Department of Energy through grant no. DE-SC0018835.

Supporting Information Available: The full citation for reference 107 and the details of the DFT computations done in support of the spectroscopy presented here, including the structures, energetics, and vibrational frequencies for each of the complexes considered. This material is available free of charge via the internet at <http://pubs.acs.org>.

REFERENCES

- 1) Marcus, Y. *Ion Solvation*, John Wiley and Sons, Chichester, UK, 1985.
- 2) Richens, D. T. *The Chemistry of Aqua Ions*, John Wiley, Chichester, U.K., 1997.
- 3) Burgess, J. *Ions in Solution*, Horwood Publishing, Chichester, UK, 1999.
- 4) Marcus, Y. *Ions in Solution and their Solvation*, John Wiley & Sons, Hoboken, NJ, 2015.
- 5) Kebarle, P. Ion Thermochemistry and Solvation from Gas-Phase Ion Equilibria. *Annu. Rev. Phys. Chem.* **1977**, *28*, 445–476.
- 6) Magnera, T. F.; David, D. E.; Michl, J. Gas-Phase Water and Hydroxyl Binding-Energies for Monopositive 1st Row Transition-Metal Ions. *J. Am. Chem. Soc.* **1989**, *111*, 4100–4101.
- 7) Marinelli, P. J.; Squires, R. R. Sequential Solvation of Atomic Transition Metal Ions - The Second Solvent Molecule Can Bind More Strongly than the First. *J. Am. Chem. Soc.* **1989**, *111*, 4101–4103.
- 8) Jayaweera, P.; Blades, A. T.; Ikononou, M. G.; Kebarle, P. Production and Study in the Gas Phase of Multiply Charged Solvated or Coordinated Metal Ions. *J. Am. Chem. Soc.* **1990**, *112*, 2452–2454.
- 9) Dalleska, N. F.; Honma, K.; Sunderlin, L. S.; Armentrout, P. B. Solvation of Transition-Metal Ions by Water - Sequential Binding Energies of $M^+(H_2O)_x$, ($x=1-4$) for $M = Ti$ to Cu Determined by Collision-Induced Dissociation. *J. Am. Chem. Soc.* **1994**, *116*, 3519–3528.
- 10) Beyer, M.; Williams, E. R.; Bondybey, V. E. Unimolecular Reactions of Dihydrated Alkaline Earth Metal Dications $M^{2+}(H_2O)_2$, $M = Be, Mg, Ca, Sr, \text{ and } Ba$: Salt-bridge

- Mechanism in the Proton-Transfer Reaction $M^{2+}(H_2O)_2 \rightarrow MOH^+ + H_3O^+$. *J. Am. Chem. Soc.* **1999**, *121*, 1565–1573.
- 11) Rodriquez-Cruz, S. E.; Jockusch, R. A.; Williams, E. R. Binding Energies of Hexahydrated Alkaline Earth Metal Ions, $M^{2+}(H_2O)_6$, $M = Mg, Ca, Sr, Ba$: Evidence of Isomeric Structures for Magnesium. *J. Am. Chem. Soc.* **1999**, *121*, 1986–1987.
 - 12) Rodriquez-Cruz, S. E.; Jockusch, R. A.; Williams, E. R. Hydration Energies and Structures of Alkaline Earth Metal Ions, $M^{2+}(H_2O)_n$, $n = 5-7$, $M = Mg, Ca, Sr$ and Ba ," *J. Am. Chem. Soc.* **1999**, *121*, 8898–8906.
 - 13) Schröder, D.; Schwarz, H. Generation, Stability, and Reactivity of Small, Multiply Charged Ions in the Gas Phase. *J. Phys. Chem. A* **1999**, *103*, 7385–7394.
 - 14) Peschke, M.; Blades, A. T.; Kebarle, P. Binding Energies for Doubly-Charged Ions $M^{2+} = Mg^{2+}, Ca^{2+}$, and Zn^{2+} with the Ligands $L = H_2O$, Acetone and N-methylacetamide in Complexes ML_n^{2+} for $n = 1$ to 7 from Gas Phase Equilibria Determinations and Theoretical Calculations. *J. Am. Chem. Soc.* **2000**, *122*, 10440–10449.
 - 15) Amicangelo, J. C.; Armentrout, P. B. Absolute Binding Energies of Alkali-Metal Cation Complexes with Benzene Determined by Threshold Collision-Induced Dissociation Experiments and Ab Initio Theory. *J. Phys. Chem. A* **2000**, *104*, 11420–11432.
 - 16) Bondybey, V. E.; Beyer, M. K. How Many Molecules Make a Solution? *Int. Rev. Phys. Chem.* **2002**, *21*, 277–306.
 - 17) Poisson, L.; Pradel, P.; Lepetit, F.; Reau, F.; Mestdagh, J. M.; Visticot, J. P. Binding Energies of First and Second Shell Water Molecules in the $Fe(H_2O)_2^+$, $Co(H_2O)_2^+$ and $Au(H_2O)_2^+$ Cluster Ions. *Eur. Phys. J. D* **2001**, *14*, 89–95.
 - 18) Stace, A. J. Metal Ion Solvation in the Gas Phase: The Quest for Higher Oxidation States. *J. Phys. Chem. A* **2002**, *106*, 7993–8005.

- 19) Armentrout, P. B. Guided Ion Beam Studies of Transition Metal-Ligand Thermochemistry. *Int. J. Mass Spectrom.* **2003**, *227*, 289–302.
- 20) Beyer, M. K. Hydrated Metal Ions in the Gas Phase. *Mass Spectrom. Rev.* **2007**, *26*, 517–541.
- 21) Polfer, N. C.; Oomens, J. Vibrational Spectroscopy of Bare and Solvated Ionic Complexes of Biological Relevance. *Mass Spectrom. Rev.* **2009**, *28*, 468–494.
- 22) Cooper, T. E.; Carl, D. R.; Armentrout, P. B. Hydration Energies of Zinc (II): Threshold Collision-Induced Dissociation Experiments and Theoretical Studies. *J. Phys. Chem. A* **2009**, *113*, 13727–13741.
- 23) Cooper, T. E.; O'Brien, J. T.; Williams, E. R.; Armentrout, P. B. Zn^{2+} Has a Primary Hydration Sphere of Five: IR Action Spectroscopy and Theoretical Studies of Hydrated Zn^{2+} Complexes in the Gas Phase. *J. Phys. Chem. A* **2010**, *114*, 12646–12655.
- 24) Van der Linde, C.; Hemmann, S.; Höckendorf, R. F.; Balaj, O. P.; Beyer, M. K. Reactivity of Hydrated Monovalent First Row Transition Metal Ions $M^+(H_2O)_n$ $M=V, Cr, Mn, Fe, Co, Ni, Cu, Zn$, toward Molecular Oxygen, Nitrous Oxide and Carbon Dioxide. *J. Phys. Chem. A* **2013**, *117*, 1011–1020.
- 25) Rogers, M. T.; Armentrout, P. B. Cationic Noncovalent Interactions: Energetics and Periodic Trends. *Chem. Rev.* **2016**, *116*, 5642–5687.
- 26) Rosi, M.; Bauschlicher, C. W., Jr. The Binding Energies of One and Two Water-Molecules to the 1st Transition-Row Metal Positive-Ions. *J. Chem. Phys.* **1989**, *90*, 7264–7272.
- 27) Rosi, M.; Bauschlicher, C. W., Jr. The Binding Energies of One and Two Water-Molecules to the 1st Transition-Row Metal Positive-Ions. II. *J. Chem. Phys.* **1990**, *92*, 1876–1878.

- 28) Bauschlicher, C. W., Jr.; Sodupe, M.; Partridge, H. A Theoretical Study of the Positive and Dipositive Ions of $M(\text{NH}_3)_n$ and $M(\text{H}_2\text{O})_n$ for $M = \text{Mg}, \text{Ca},$ or Sr . *J. Chem. Phys.* **1992**, *96*, 4453–4463.
- 29) Feller, D.; Glendening, E. D.; Kendall, R. A.; Peterson, K. A. An Extended Basis-Set Ab-Initio Study of $\text{Li}^+(\text{H}_2\text{O})_n$, $n=1-6$. *J. Chem. Phys.* **1994**, *100*, 4981–4997.
- 30) Feller, D.; Glendening, E. D.; Woon, D. E.; Feyereisen, M. W. An Extended Basis-Set Ab-Initio Study of Alkali-Metal Cation-Water Clusters. *J. Chem. Phys.* **1995**, *103*, 3526–3542.
- 31) Glendening, E. D.; Feller, D. Cation Water Interactions - the $M^+(\text{H}_2\text{O})_n$ Clusters for Alkali-Metals, $M = \text{Li}, \text{Na}, \text{K}, \text{Rb},$ and Cs . *J. Phys. Chem.* **1995**, *99*, 3060–3067.
- 32) Watanabe, H.; Iwata, S.; Hashimoto, K.; Misaizu, F.; Fuke, K. Molecular-Orbital Studies of the Structures and Reactions of Singly Charged Magnesium-Ion with Water Clusters, $\text{Mg}^+(\text{H}_2\text{O})_n$. *J. Am. Chem. Soc.* **1995**, *117*, 755–763.
- 33) Wasserman, E.; Rustad, R. R.; Xantheas, S. S. Interaction Potential of Al^{3+} in Water from First Principles Calculations. *J. Chem. Phys.* **1997**, *106*, 9769–9780.
- 34) Tsurusawa, T.; Iwata, S. Theoretical Studies of Structures and Ionization Threshold Energies of Water Cluster Complexes with a Group 1 Metal, $M(\text{H}_2\text{O})_n$ ($M = \text{Li}$ and Na). *J. Phys. Chem. A* **1999**, *103*, 6134–6141.
- 35) Irigoras, A.; Elizalde, O.; Silanes, I.; Fowler, J. E.; Ugalde, J. M. Reactivity of $\text{Co}^+(^3\text{F}, ^5\text{F})$, $\text{Ni}^+(^2\text{D}, ^4\text{F})$ and $\text{Cu}^+(^1\text{S}, ^3\text{D})$: Reaction of Co^+ , Ni^+ and Cu^+ with Water. *J. Am. Chem. Soc.* **2000**, *122*, 114–122.
- 36) Tsurusawa, T.; Iwata, S. Electron-Hydrogen Bonds and OH Harmonic Frequency Shifts in Water Cluster Complexes with a Group 1 Metal Atom, $M(\text{H}_2\text{O})_n$ ($M = \text{Li}$ and Na). *J. Chem. Phys.* **2000**, *112*, 5705–5710.

- 37) Lee, E. C.; Lee, H. M.; Tarakeshwar, P.; Kim, K. S. Structures, Energies, and Spectra of Aqua-Silver (I) Complexes. *J. Chem. Phys.* **2003**, *119*, 7725–7736.
- 38) Mercero, J. M.; Maxtain, J. M.; Lopez, X.; York, D. M.; Largo, A.; Eriksson, L. A.; Ugalde, J. M. Theoretical Methods that Help Understanding the Structure and Reactivity of Gas Phase Ions. *Int. J. Mass Spectrom.* **2005**, *240*, 37–99.
- 39) Kolaski, M.; Lee, H. M.; Choi, Y. C.; Kim, K. S.; Tarakeshwar, P.; Miller, D. J.; Lisý, J. M. Structures, Energetics and Spectra of Aqua-Cesium (I) Complexes: An Ab Initio and Experimental Study. *J. Chem. Phys.* **2007**, *126*, 074302.
- 40) Pandelov, S.; Werhahn, J. C.; Pilles, B. M.; Xantheas, S. S.; Iglev, H. An Empirical Correlation between the Enthalpy of Solution of Aqueous Salts and Their Ability to Form Hydrates. *J. Phys. Chem. A* **2010**, *114*, 10454–10457.
- 41) Garza-Galindo, R.; Castro, M.; Duncan, M. A. Theoretical Study of Nascent Hydration in the $\text{Fe}^+(\text{H}_2\text{O})_n$ System. *J. Phys. Chem. A* **2012**, *116*, 1906–1913.
- 42) Miliordos, E.; Xantheas, S. S. Elucidating the Mechanism Behind the Stabilization of Multi-Charged Metal Cations in Water: A Case Study of the Electronic States of Microhydrated Mg^{2+} , Ca^{2+} and Al^{3+} . *Phys. Chem. Chem. Phys.* **2014**, *16*, 6886–6892.
- 43) Miliordos, E.; Xantheas, S. S. Unimolecular and Hydrolysis Channels for the Detachment of Water from Microsolvated Alkaline Earth Dication (Mg^{2+} , Ca^{2+} , Sr^{2+} , Ba^{2+}) Clusters. *Theor. Chem. Acc.* **2014**, *133*, 1450.
- 44) Lessen, D. E.; Asher, R. L.; Brucat, P. J. Vibrational Structure of an Electrostatically Bound Ion-Water Complex. *J. Chem. Phys.* **1990**, *93*, 6102–6103.
- 45) Willey, K. F.; Yeh, C. S.; Robbins, D. L.; Pilgrim, J. S.; Duncan, M. A. Photodissociation Spectroscopy of $\text{Mg}^+-\text{H}_2\text{O}$ and $\text{Mg}^+-\text{D}_2\text{O}$. *J. Chem. Phys.* **1992**, *97*, 8886–8895.

- 46) Scurlock, C. T.; Pullins, S. H.; Reddic, J. E.; Duncan, M. A. Photodissociation Spectroscopy of $\text{Ca}^+\text{-H}_2\text{O}$ and $\text{Ca}^+\text{-D}_2\text{O}$. *J. Chem. Phys.* **1996**, *104*, 4591–4599.
- 47) Sanekata, M.; Misaizu, F.; Fuke, K. Photodissociation Study on $\text{Ca}^+(\text{H}_2\text{O})_n$, $n = 1\text{--}6$: Electron Structure and Photoinduced Dehydrogenation Reaction. *J. Chem. Phys.* **1996**, *104*, 9768–9778.
- 48) Duncan, M. A. Spectroscopy of Metal Ion Complexes: Gas Phase Models for Solvation. *Annu. Rev. Phys. Chem.* **1997**, *48*, 69–93.
- 49) Wang, K. H.; Rodham, D. A.; McKoy, V.; Blake, G. A. High-Resolution Zero-Kinetic-Energy Pulsed Field Ionization, Photoelectron Spectra of the $\text{Na}(\text{H}_2\text{O})$ Complex. *J. Chem. Phys.* **1998**, *108*, 4817–4827.
- 50) Agreiter, J. K.; Knight, A.M.; Duncan, M. A. ZEKE-PFI Spectroscopy of the $\text{Al}(\text{H}_2\text{O})$ and $\text{Al}(\text{D}_2\text{O})$ Complexes. *Chem. Phys. Lett.* **1999**, *313*, 162–170.
- 51) Fuke, K.; Hashimoto, K.; Iwata, S. Structures, Spectroscopies, and Reactions of Atomic Ions with Water Clusters. *Adv. Chem. Phys.* **1999**, *110*, 431–523.
- 52) Duncan, M. A. Frontiers in the Spectroscopy of Mass-Selected Molecular Ions. *Int. J. Mass Spectrom.* **2000**, *200*, 545–569.
- 53) Farrar, J. M. Size-Dependent Reactivity in Open Shell Metal-Ion Polar Solvent Clusters: Spectroscopic Probes of Electronic-Vibration Coupling, Oxidation and Ionization. *Int. Rev. Phys. Chem.* **2003**, *22*, 593–640.
- 54) Abate, Y.; Kleiber, P. D. Photodissociation Spectroscopy of $\text{Zn}^+(\text{H}_2\text{O})$ and $\text{Zn}^+(\text{D}_2\text{O})$. *J. Chem. Phys.* **2005**, *122*, 084305.
- 55) Cox, H.; Stace, A. J. Recent Advances in the Visible and UV Spectroscopy of Metal Dication Complexes. *Int. Rev. Phys. Chem.* **2010**, *29*, 555–588.

- 56) Daluz, J. S.; Kocak, A.; Metz, R. B. Photodissociation Studies of the Electronic and Vibrational Spectroscopy of $\text{Ni}^+(\text{H}_2\text{O})$. *J. Phys. Chem. A* **2012**, *116*, 1344–1352.
- 57) Kocak, A.; Austein-Miller, G.; Pearson III, W. L.; Gokhan, A.; Metz, R. B. Dissociation Energy and Electronic and Vibrational Spectroscopy of $\text{Co}^+(\text{H}_2\text{O})$ and its Isotopomers. *J. Phys. Chem. A* **2013**, *117*, 1254–1264.
- 58) Pearson, W. L., III; Copeland, C.; Kocak, A.; Sallese, Z.; Metz, R. B. Near Ultraviolet Photodissociation Spectroscopy of $\text{Mn}^+(\text{H}_2\text{O})$ and $\text{Mn}^+(\text{D}_2\text{O})$. *J. Chem. Phys.* **2014**, *141*, 204305.
- 59) Lisy, J. M. Spectroscopy and Structure of Solvated Alkali-Metal Ions. *Int. Rev. Phys. Chem.* **1997**, *16*, 267–289.
- 60) Walters, R. S.; Walker, N. R.; Pillai, E. D.; Duncan, M. A. Infrared Spectroscopy of $\text{V}^+(\text{H}_2\text{O})$ and $\text{V}^+(\text{D}_2\text{O})$ Complexes: Ligand Deformation and an Incipient Reaction. *J. Chem. Phys.* **2003**, *119*, 10471–10474.
- 61) Walters, R. S.; Duncan, M. A. Infrared Spectroscopy of Solvation and Isomers in $\text{Fe}^+(\text{H}_2\text{O})_{1,2}\text{Ar}_m$ Complexes. *Aust. J. Chem.* **2004**, *57*, 1145–1148.
- 62) Inokuchi, Y.; Ohshimo, K.; Misaizu, F.; Nishi, N. Structures of $[\text{Mg}(\text{H}_2\text{O})_{1,2}]^+$ and $[\text{Al}(\text{H}_2\text{O})_{1,2}]^+$ Ions Studied by Infrared Photodissociation Spectroscopy: Evidence of $[\text{HO-Al-H}]^+$ Ion Core Structure in $[\text{Al}(\text{H}_2\text{O})_2]^+$. *Chem. Phys. Lett.* **2004**, *390*, 140–144.
- 63) Inokuchi, Y.; Ohshimo, K.; Misaizu, F.; Nishi, N. Infrared Photodissociation Spectroscopy of $[\text{Mg}(\text{H}_2\text{O})_{1-4}]^+$ and $[\text{Mg}(\text{H}_2\text{O})_{1-4}\text{Ar}]^+$. *J. Phys. Chem. A* **2004**, *108*, 5034–5040.
- 64) Walker, N. R.; Walters, R. S.; Tsai, M. K.; Jordan, K. D.; Duncan, M. A. Infrared Photodissociation Spectroscopy of $\text{Mg}^+(\text{H}_2\text{O})\text{Ar}_n$ Complexes: Isomers in Progressive Microsolvation. *J. Phys. Chem. A* **2005**, *109*, 7057–7067.

- 65) Walters, R. S.; Pillai, E. D.; Duncan, M. A. Solvation Dynamics in $\text{Ni}^+(\text{H}_2\text{O})_n$ Clusters Probed with Infrared Spectroscopy. *J. Am. Chem. Soc.* **2005**, *127*, 16599–16610.
- 66) Vaden, T. D.; Lisy, J. M.; Carnegie, P. D.; Pillai, E. D.; Duncan, M. A. Infrared Spectroscopy of the $\text{Li}^+(\text{H}_2\text{O})_n$ Complex: The Role of Internal Energy and its Dependence on Ion Preparation. *Phys. Chem. Chem. Phys.* **2006**, *8*, 3078–3082.
- 67) Iino, T.; Ohashi, K.; Inoue, K.; Judai, K.; Nishi, N.; Sekiya, H. Infrared Spectroscopy of $\text{Cu}^+(\text{H}_2\text{O})_n$ and $\text{Ag}^+(\text{H}_2\text{O})_n$: Coordination and Solvation of Noble-Metal Ions. *J. Chem. Phys.* **2007**, *126*, 194302–194313.
- 68) Carnegie, P. D.; Bandyopadhyay, B.; Duncan, M. A. Infrared Spectroscopy of $\text{Cr}^+(\text{H}_2\text{O})$ and $\text{Cr}^{2+}(\text{H}_2\text{O})$: The Role of Charge in Cation Hydration. *J. Phys. Chem. A* **2008**, *112*, 6237–6243.
- 69) Bush, M. F.; Saykally, R. J.; Williams, E. R. Reactivity and Infrared Spectroscopy of Gaseous Hydrated Trivalent Metal Ions. *J. Am. Chem. Soc.* **2008**, *130*, 9122–9128.
- 70) Bush, M. F.; Saykally, R. J.; Williams, E. R. Infrared Action Spectroscopy of $\text{Ca}^{2+}(\text{H}_2\text{O})_{11-69}$ Exhibit Spectral Signatures for Condensed-Phase Structures with Increasing Cluster Size. *J. Am. Chem. Soc.* **2008**, *130*, 15482–15489.
- 71) Bush, M. F.; O'Brien, J. T.; Prell, J. S.; Wu, C.-C.; Saykally, R. J.; Williams, E. R. Hydration of Alkaline Earth Metal Dications: Effects of Metal Ion Size Determined Using Infrared Action Spectroscopy. *J. Am. Chem. Soc.* **2009**, *131*, 13270–13277.
- 72) Sasaki, J.; Ohashi, K.; Inoue, K.; Imamura, T.; Judai, K.; Nishi, N.; Sekiya, H. Infrared Photodissociation Spectroscopy of $\text{V}^+(\text{H}_2\text{O})_n$ ($n = 2-8$): Coordinative Saturation of V^+ with Four H_2O Molecules. *Chem. Phys. Lett.* **2009**, *474*, 36–40.

- 73) Carnegie, P. D.; McCoy, A. B.; Duncan, M. A. Infrared Spectroscopy and Theory of $\text{Cu}^+(\text{H}_2\text{O})\text{Ar}_2$ and $\text{Cu}^+(\text{D}_2\text{O})\text{Ar}_2$: Fundamentals and Combination Bands. *J. Phys. Chem. A* **2009**, *113*, 4849–4854.
- 74) Carnegie, P. D.; Bandyopadhyay, B.; Duncan, M. A. Infrared Spectroscopy of $\text{Sc}^+(\text{H}_2\text{O})$ and $\text{Sc}^{2+}(\text{H}_2\text{O})$ via Argon Complex Predissociation: The Charge Dependence in Cation Hydration. *J. Chem. Phys.* **2011**, *134*, 014302.
- 75) Carnegie, P. D.; Bandyopadhyay, B.; Duncan, M. A. Infrared Spectroscopy of $\text{Mn}^+(\text{H}_2\text{O})_n$ and $\text{Mn}^{2+}(\text{H}_2\text{O})$ Complexes via Argon Complex Predissociation. *J. Phys. Chem. A* **2011**, *115*, 7602–7609.
- 76) Beck, J. P.; Lisy, J. M. Infrared Spectroscopy of Hydrated Alkali Metal Cations: Evidence of Multiple Photon Absorption. *J. Chem. Phys.* **2011**, *135*, 044302.
- 77) Furukawa, K.; Ohashi, K.; Koga, N.; Imamura, T.; Judai, K.; Nishi, N.; Sekiya, H. Coordinatively Unsaturated Cobalt Ion in $\text{Co}^+(\text{H}_2\text{O})_n$ ($n = 4-6$) Probed with Infrared Photodissociation Spectroscopy. *Chem. Phys. Lett.* **2011**, *508*, 202–206.
- 78) O'Brien, J.T.; Williams, E. R. Coordination Numbers of Hydrated Divalent Transition Metal Ions Investigated with IRPD Spectroscopy. *J. Phys. Chem. A* **2011**, *115*, 14612–14619.
- 79) Prell, J. S.; O'Brien, J. T.; Williams, E. R. Structural and Electronic Field Effects of Ions in Aqueous Nanodroplets. *J. Am. Chem. Soc.* **2011**, *133*, 4810–4818.
- 80) Li, Y.; Wang, G.; Zhou, M. Coordination and Solvation of the Au^+ Cation: Infrared Photodissociation Spectroscopy of Mass-Selected $\text{Au}(\text{H}_2\text{O})_n^+$ ($n = 1-8$) Complexes. *J. Phys. Chem. A* **2012**, *116*, 10793–10801.
- 81) Bandyopadhyay, B.; Duncan, M. A. Infrared Spectroscopy of $\text{V}^{2+}(\text{H}_2\text{O})$ Complexes. *Chem. Phys. Lett.* **2012**, *530*, 10–15.

- 82) Bandyopadhyay, B.; Reishus, K. N.; Duncan, M. A. Infrared Spectroscopy of Solvation in Small $\text{Zn}^+(\text{H}_2\text{O})_n$ Complexes. *J. Phys. Chem. A* **2013**, *117*, 7794–7803.
- 83) Marsh, B. M.; Zhou, J.; Garand, E. Vibrational Spectroscopy of Small Hydrated CuOH^+ Clusters. *J. Phys. Chem. A* **2014**, *118*, 2063–2017.
- 84) Johnson, C. J.; Dzugan, L. C.; Wolk, A. B.; Leavitt, C. M.; Fournier, J. A.; McCoy, A. B.; Johnson, M. A. Microhydration of Contact Ion Pairs in $\text{M}^{2+}\text{OH}^-(\text{H}_2\text{O})_{n=1-5}$ (M = Mg, Ca) Clusters: Spectral Manifestations of a Mobile Proton Defect in the First Hydration Sphere. *J. Phys. Chem. A* **2014**, *118*, 7590–7597.
- 85) Ward, T. B.; Carnegie, P. D.; Duncan, M. A. Infrared Spectroscopy of the $\text{Ti}(\text{H}_2\text{O})\text{Ar}^+$ Ion-Molecule Complex: Electronic State Switching Induced by Argon. *Chem. Phys. Lett.* **2016**, *654*, 1–5.
- 86) Ward, T. B.; Miliordos, E.; Carnegie, P. D.; Xantheas, S. S.; Duncan, M. A. Ortho-Para Interconversion in Cation-Water Complexes: The Case of $\text{V}^+(\text{H}_2\text{O})$ and $\text{Nb}^+(\text{H}_2\text{O})$ Clusters. *J. Chem. Phys.* **2017**, *146*, 224305.
- 87) Duncan, M. A. Laser Vaporization Cluster Sources. *Rev. Sci. Instrum.* **2012**, *83*, 041101.
- 88) LaiHing, K.; Taylor, T. G.; Cheng, P. Y.; Willey, K. F.; Peschke, M.; Duncan, M. A. Photodissociation in a Reflectron Time-of-Flight Mass Spectrometer: A Novel MS/MS Scheme for High Mass Systems. *Anal. Chem.* **1989**, *61*, 1458–1460.
- 89) Duncan, M. A. Reflectron Time-of-Flight Mass Spectrometer for Laser Photodissociation. *Rev. Sci. Instrum.* **1992**, *63*, 2177–2186.
- 90) Bosenberg, W. R.; Guyer, D. R. Broadly Tunable, Single-Frequency Optical Parametric Frequency-Conversion System. *J. Opt. Soc. Am. B* **1993**, *10*, 1716–1722.
- 91) Okumura, M.; Yeh, L. I.; Myers, J. D.; Lee, Y. T. Infrared Spectra of the Cluster Ions $\text{H}_7\text{O}_3^+-\text{H}_2$ and $\text{H}_9\text{O}_4^+-\text{H}_2$. *J. Chem. Phys.* **1986**, *85*, 2328–2329.

- 92) Okumura, M.; Yeh, L. I.; Myers, J. D.; Lee, Y. T. Infrared Spectra of the Solvated Hydronium Ion: Vibrational Predissociation Spectroscopy of Mass-Selected $\text{H}_3\text{O}^+(\text{H}_2\text{O})_n(\text{H}_2)_m$. *J. Phys. Chem.* **1990**, *94*, 3416–3427.
- 93) Yeh, L. I.; Okumura, M.; Myers, J. D.; Price, J. M.; Lee, Y. T. Vibrational Spectroscopy of the Hydrated Hydronium Cluster Ions $\text{H}_3\text{O}^+(\text{H}_2\text{O})_n$ ($n = 1,2,3$). *J. Chem. Phys.* **1989**, *91*, 7319–7330.
- 94) Ebata, T.; Fujii, A.; Mikami, N. Vibrational Spectroscopy of Small-Sized Hydrogen-Bonded Clusters and Their Ions. *Int. Rev. Phys. Chem.* **1998**, *17*, 331–361.
- 95) Bieske, E. J.; Dopfer, O. High-Resolution Spectroscopy of Cluster Ions. *Chem. Rev.* **2000**, *100*, 3963–3998.
- 96) Robertson, W. H.; Johnson, M. A. Molecular Aspects of Halide Hydration: The Cluster Approach. *Annu. Rev. Phys. Chem.* **2003**, *54*, 173–213.
- 97) Duncan, M. A. Infrared Spectroscopy to Probe Structure and Dynamics in Metal Ion-Molecule Complexes. *Int. Rev. Phys. Chem.* **2003**, *22*, 407–435.
- 98) Rizzo, T. R.; Stearns, J. A.; Boyarkin, O. V. Spectroscopic Studies of Cold, Gas-Phase Biomolecular Ions. *Int. Rev. Phys. Chem.* **2009**, *28*, 481–515.
- 99) Baer, T.; Dunbar, R. C. Ion Spectroscopy: Where Did It Come From, Where Is It Now, and Where Is It Going? *J. Am. Soc. Mass. Spectrom.* **2010**, *21*, 681–693.
- 100) Redwine, J. G.; Davis, Z. A.; Burke, N. L.; Oglesbee, R. A.; McLuckey, S. A.; Zwier, T. S. A Novel Ion Trap Based Tandem Mass Spectrometer for the Spectroscopic Study of Cold Gas Phase Polyatomic Ions. *Int. J. Mass Spectrom.* **2013**, *348*, 9–14.
- 101) Chakrabarty, S.; Holtz, M.; Campbell, E. K.; Banerjee, A.; Gerlich, D.; Maier, J. P. A Novel Method to Measure Electronic Spectra of Cold Molecular Ions. *J. Phys. Chem. Lett.* **2013**, *4*, 4051–4054.

- 102) Wolk, A. B.; Leavitt, C. M.; Garand, E.; Johnson, M. A. Cryogenic Ion Chemistry and Spectroscopy. *Acc. Chem. Res.* **2014**, *47*, 202–210.
- 103) Heine, N.; Asmis, K. R. Cryogenic Ion Trap Vibrational Spectroscopy of Hydrogen-Bonded Clusters Relevant to Atmospheric Chemistry. *Int. Rev. Phys. Chem.* **2015**, *34*, 1–34.
- 104) Roithová, J.; Gray, A.; Andris, E.; Jašík, J.; Gerlich, D. Helium Tagging Infrared Photodissociation Spectroscopy of Reactive Ions. *Acc. Chem. Res.* **2016**, *49*, 223–230.
- 105) Zheng, H. J.; Yang, N.; Johnson, M. A. Advances in Ion Spectroscopy: From Astrophysics to Biology. *Faraday Discuss.* **2019**, *217*, 8–33.
- 106) Schwarz, H.; Asmis, K. R. Identification of Active Sites and Structural Characterization of Reactive Ionic Intermediates by Cryogenic Ion Trap Vibrational Spectroscopy. *Chem. Eur. J.* **2019**, *25*, 2112–2126.
- 107) Frisch, M. J. et al., *Gaussian 03* (Revision B.02), Gaussian, Inc., Pittsburgh PA, 2003.
- 108) Scott, A. P.; Radom, L. Harmonic Vibrational Frequencies: An Evaluation of Hartree-Fock, Møller-Plesset, Quadratic Configuration Interaction, Density Functional Theory, and Semi-Empirical Scale Factors. *J. Phys. Chem.* **1996**, *100*, 16502–16513.
- 109) Shimanouchi, T. Molecular Vibrational Frequencies, in *NIST Chemistry Webbook*, NIST Standard Reference Database Number 69, Eds. P.J. Linstrom and W.G. Mallard, National Institute of Standards and Technology, Gaithersburg MD, 20899 (<http://Webbook.Nist.Gov>).
- 110) Galabov, B.; Yamaguchi, Y.; Remington, R. B.; Schaefer, H. F. High Level Ab Initio Quantum Mechanical Predictions of Infrared Intensities. *J. Phys. Chem. A* **2002**, *106*, 819–832.

- 111) Walker, N. R.; Walters, R. S.; Duncan, M. A. Infrared Photodissociation Spectroscopy of $V^+(CO_2)_n$ and $V^+(CO_2)_nAr$ Complexes. *J. Chem. Phys.* **2004**, *120*, 10037–10045.
- 112) Ricks, A. M.; Reed, Z. D.; Duncan, M. A. Seven-Coordinate Homoleptic Metal Carbonyls in the Gas Phase. *J. Am. Chem. Soc.* **2009**, *131*, 9176–9177.
- 113) Ricks, A. M.; Brathwaite, A. D.; Duncan, M. A. Coordination and Spin States of $V^+(CO)_n$ Clusters Revealed by IR Spectroscopy. *J. Phys. Chem. A* **2013**, *117*, 1001–1010.
- 114) Harvey, J. N. DFT Computation of Relative Spin-State Energetics of Transition Metal Compounds. *Structure and Bonding* **2004**, *112*, 151–183.
- 115) Cramer, C. J.; Truhlar, D. J. Density Functional Theory for Transition Metals and Transition Metal Chemistry. *Phys. Chem. Chem. Phys.* **2009**, *11*, 10757–10816.
- 116) Li, S.; Hennigan, J. M.; Dixon, D. A.; Peterson, K. A. Accurate Thermochemistry for Transition Metal Oxide Clusters. *J. Phys. Chem. A* **2009**, *113*, 7861–7877.
- 117) Cohen, A. J.; Mori-Sánchez, P.; Yang, W. Challenges for Density Functional Theory. *Chem. Rev.* **2012**, *112*, 289–320.
- 118) Shil, S.; Bhattacharya, D.; Sarkar, S.; Misra, A. Performance of the Widely Used Minnesota Density Functionals for the Prediction of Heat of Formations, Ionization Potentials of Some Benchmarked First Row Transition Metal Complexes. *J. Phys. Chem. A* **2013**, *117*, 4945–4955.
- 119) McDonald II, D. C.; Wagner, J. P.; McCoy, A. B.; Duncan, M. A. Near-Infrared Spectroscopy of Protonated Water Clusters: Higher Elevations in the Hydrogen Bonding Landscape. *J. Phys. Chem. Lett.* **2018**, *9*, 5664–5671.
- 120) Shin, J.-W.; Hammer, N. I.; Diken, E. G.; Johnson, M. A.; Walters, R. S.; Jaeger, T. D.; Duncan, M. A.; Christie, R. A.; Jordan, K. D. Infrared Signature of Structural Motifs

- Associated with the $\text{H}^+(\text{H}_2\text{O})_n$, $n = 6\text{--}27$, Clusters. *Science* **2004**, *304*, 1137–1140.
- 121) Douberly, G. E.; Ricks, A. M.; Duncan, M. A. Infrared Spectroscopy of Perdeuterated Protonated Water Clusters in the Vicinity of the Clathrate Cage Structure. *J. Phys. Chem. A* **2009**, *113*, 8449–8453.
- 122) Mizuse, K.; Mikami, N.; Fujii, A. Infrared Spectra and Hydrogen-Bonded Network Structures of Large Protonated Water Clusters $\text{H}^+(\text{H}_2\text{O})_n$ ($n = 20\text{--}200$). *Angew. Chem. Int. Ed. Phys.* **2010**, *49*, 10119–10122.
- 123) Fournier, J. A.; Wolke, C. T.; Johnson, M. A.; Odbadrakh, T. T.; Jordan, K. D.; Kathmann, S. M.; Xantheas, S. S. Snapshots of Proton Accommodation at a Microscopic Water Surface: Understanding the Vibrational Spectral Signatures of the Charge Defect in Cryogenically Cooled $\text{H}^+(\text{H}_2\text{O})_{n=2-28}$ Clusters. *J. Phys. Chem. A* **2015**, *119*, 9425–9440.
- 124) Raymond, E. A.; Richmond, G. L. Probing the Molecular Structure and Bonding of the Surface of Aqueous Salt Solutions. *J. Phys. Chem. B* **2004**, *108*, 5051–5059.
- 125) Gopalakrishnan, S.; Liu, D.; Allen, H. C.; Kuo, M.; Shultz, M. J. Vibrational Spectroscopic Studies of Aqueous Interfaces: Salts, Acids, Bases, and Nanodrops. *Chem. Rev.* **2006**, *106*, 1155–1175.
- 126) Ji, N.; Ostroverkhov, V.; Tian, C. S.; Shen, Y. R. Characterization of Vibrational Resonances of Water-Vapor Interfaces by Phase-Sensitive Sum-Frequency Spectroscopy. *Phys. Rev. Lett.* **2008**, *100*, 096102.

Figure Captions

Figure 1. Infrared photodissociation spectra measured for the $V^+(H_2O)_n$ clusters for $n = 3,4,5,7$ in the mass channel corresponding to the elimination of a single water molecule.

Figure 2. Infrared photodissociation spectrum measured for the $V^+(H_2O)Ar_2$ cluster compared to those measured for the $V^+(H_2O)_nAr$ clusters for $n = 2-4$ (left) and $4-7$ (right). All are recorded in the mass channel corresponding to the elimination of an argon atom.

Figure 3. Infrared photodissociation spectrum measured for the $V^+(H_2O)Ar_2$ cluster compared to spectra predicted by density functional theory for different spin states of this ion.

Figure 4. Near-infrared photodissociation spectrum measured for the $V^+(H_2O)Ar_2$ cluster compared to anharmonic vibrational spectra predicted by density functional theory and the VPT2 method.

Figure 5. Infrared photodissociation spectrum measured for the $V^+(H_2O)_2Ar$ cluster compared to spectra predicted by density functional theory for different isomeric structures of this ion.

Figure 6. Infrared photodissociation spectrum measured for the $V^+(H_2O)_3Ar$ cluster compared to spectra predicted by density functional theory for different isomeric structures of this ion.

Figure 7. Infrared photodissociation spectrum measured for the $V^+(H_2O)_4Ar$ cluster compared to spectra predicted by density functional theory for different isomeric structures of this ion.

Figure 8. Infrared photodissociation spectrum measured for the $V^+(H_2O)_5Ar$ cluster compared to spectra predicted by density functional theory for different isomeric structures of this ion.

Figure 9. Infrared photodissociation spectrum measured for the $V^+(H_2O)_6Ar$ cluster compared to spectra predicted by density functional theory for different isomeric structures of this ion.

Figure 10. Infrared photodissociation spectra measured for the $V^+(H_2O)_{8,11,14}$ clusters measured via the elimination of one water molecule.

Figure 11. Infrared photodissociation spectra measured for the $V^+(H_2O)_{17-21}$ clusters measured via the elimination of one water molecule.

Figure 12. Infrared photodissociation spectra measured for the $V^+(H_2O)_{22-28,30}$ clusters measured via the elimination of one water molecule.

Figure 13. The spectral splitting of the surface O–H stretch in the larger clusters arising from the difference between AAD and AD coordination. The splittings for the present vanadium ion system are compared to those measured previously for nickel cation-water and protonated water clusters. Error bars (not shown) are $\pm 1 \text{ cm}^{-1}$, determined by the line widths of spectral features.

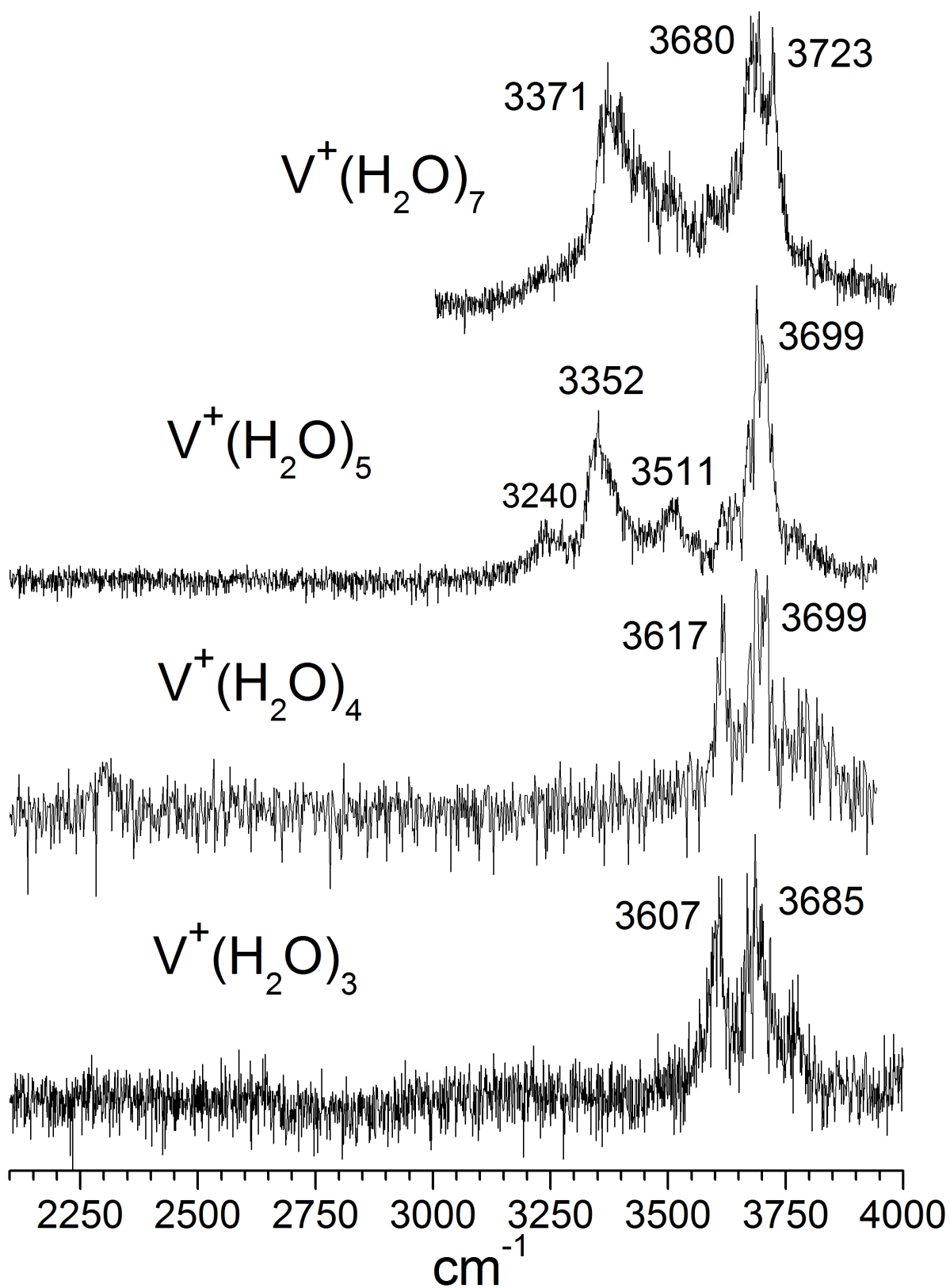


Figure 1.

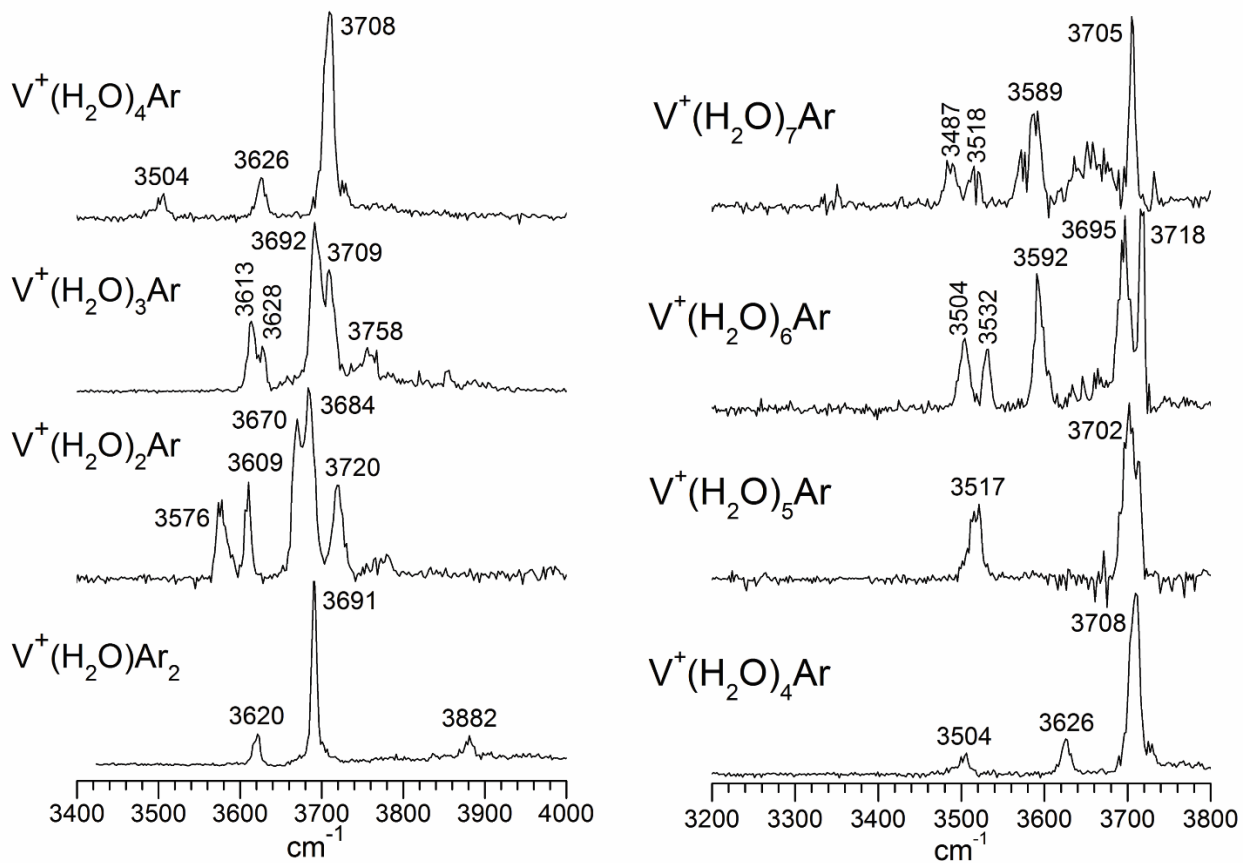


Figure 2.

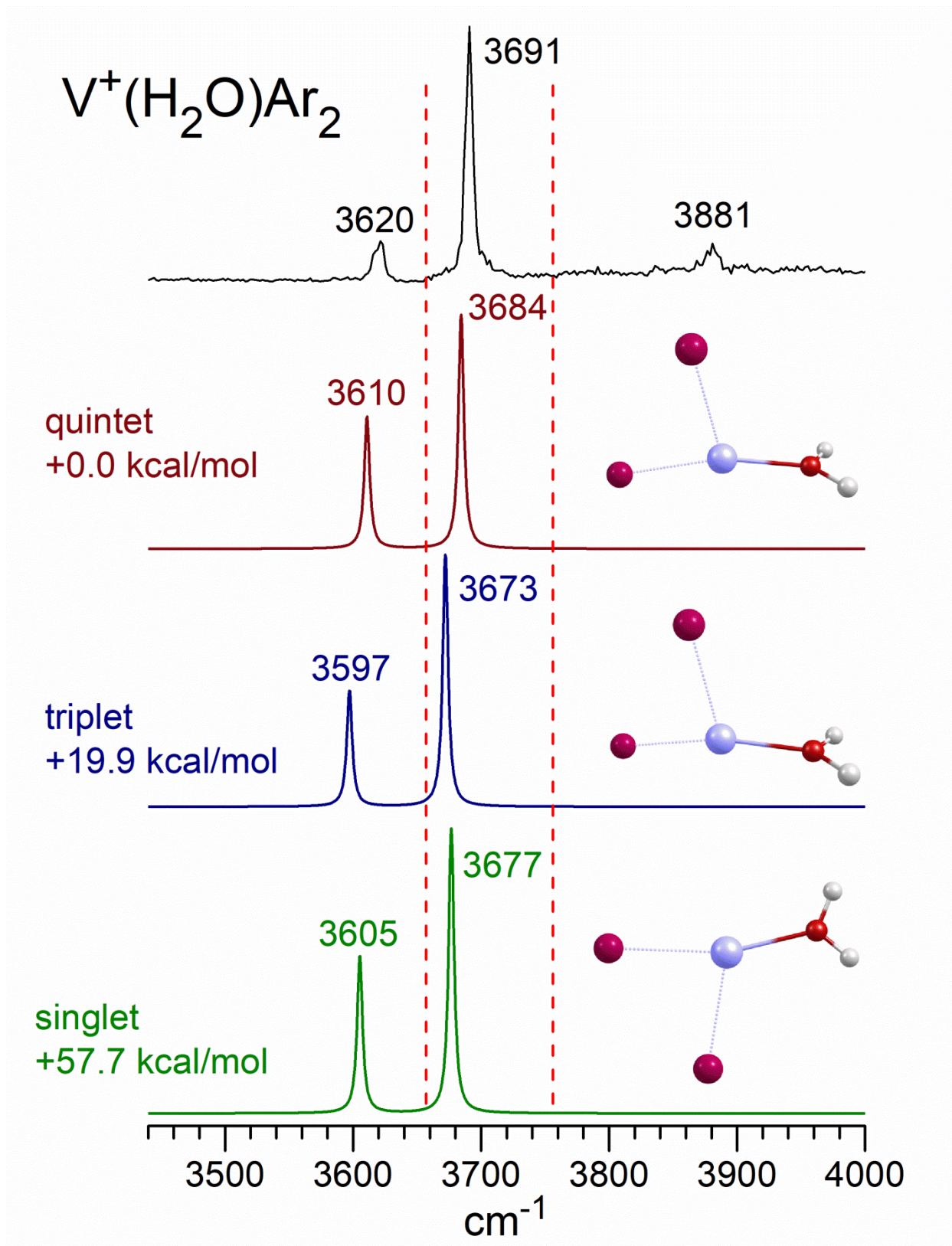


Figure 3.

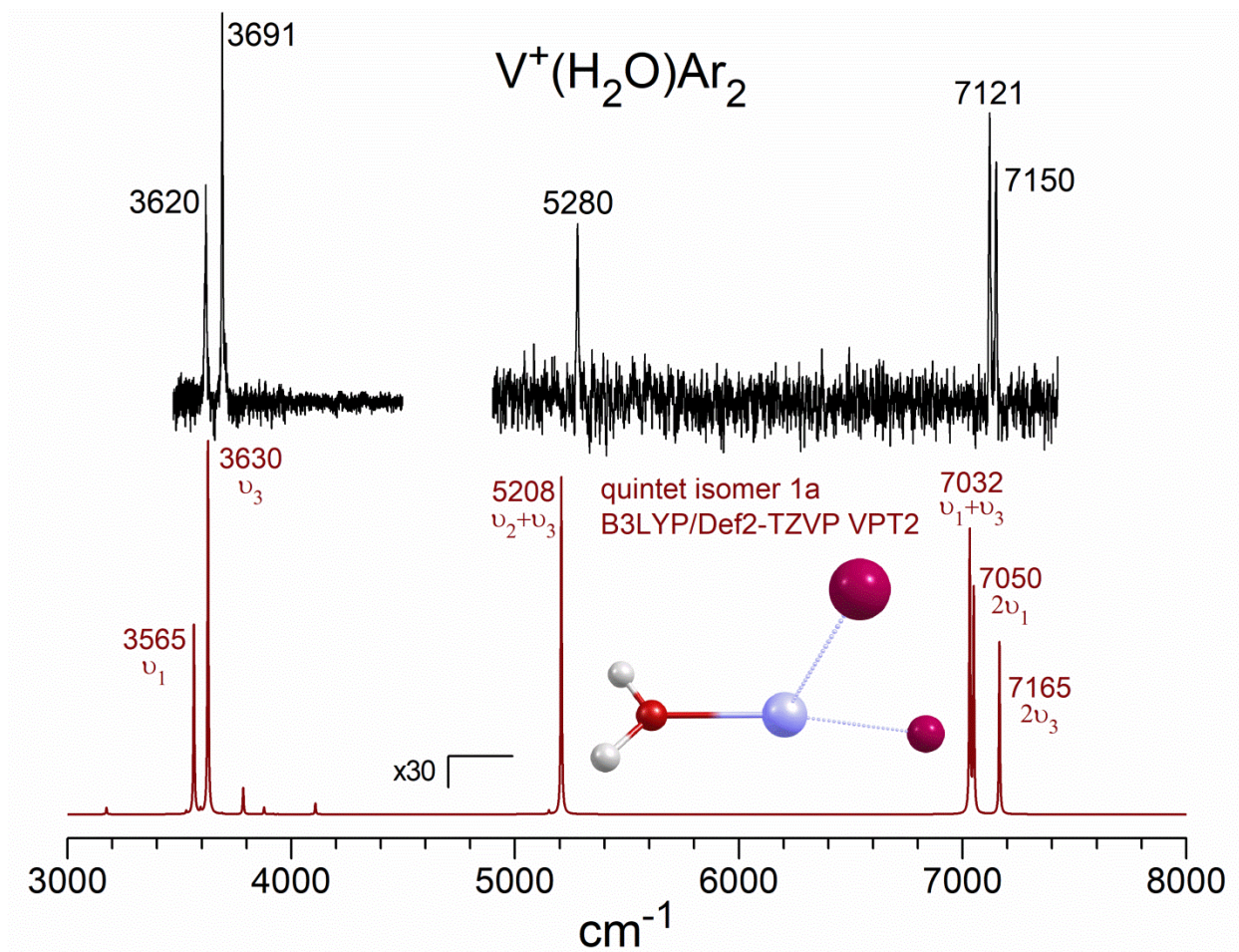


Figure 4.

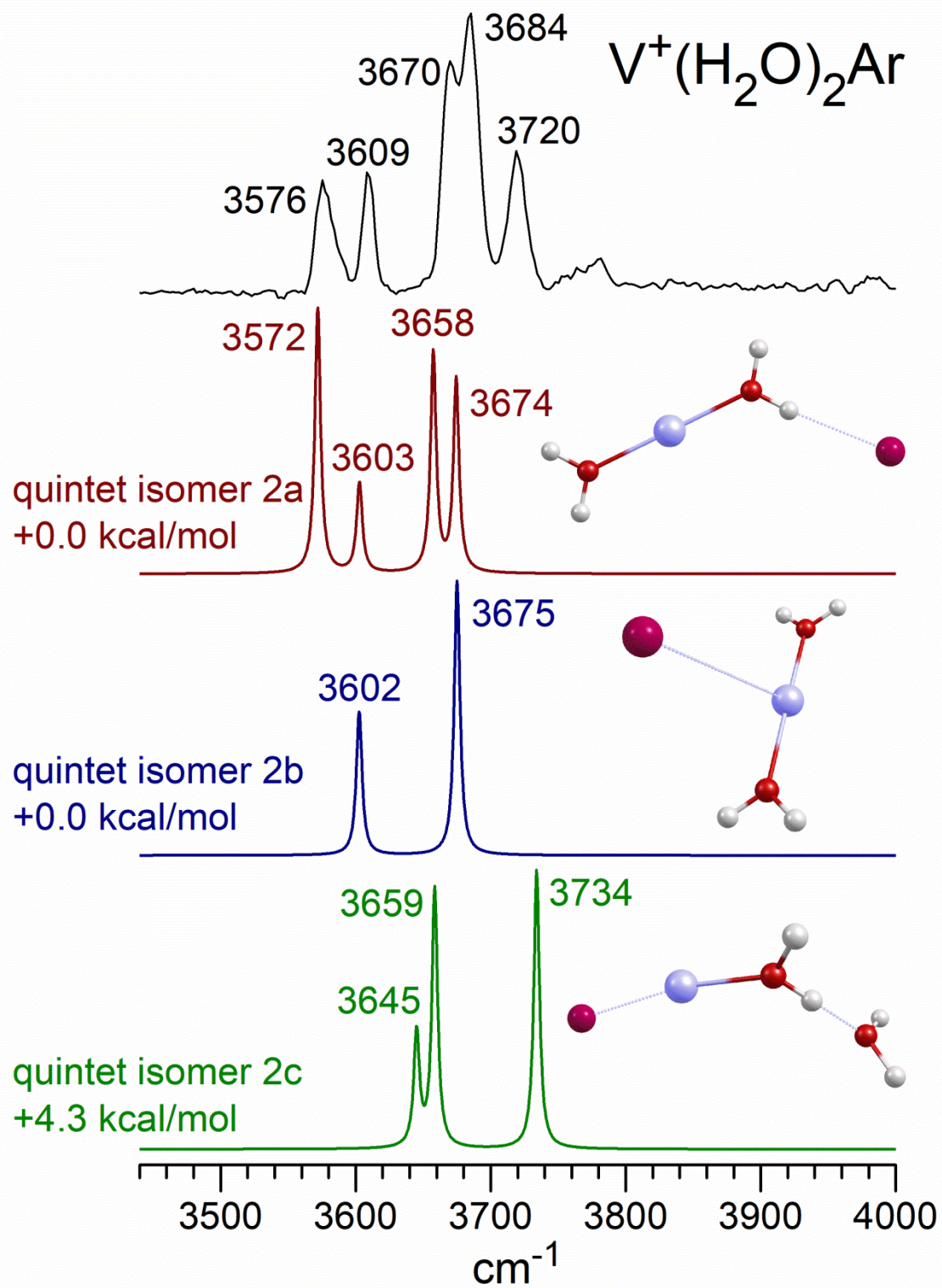


Figure 5.

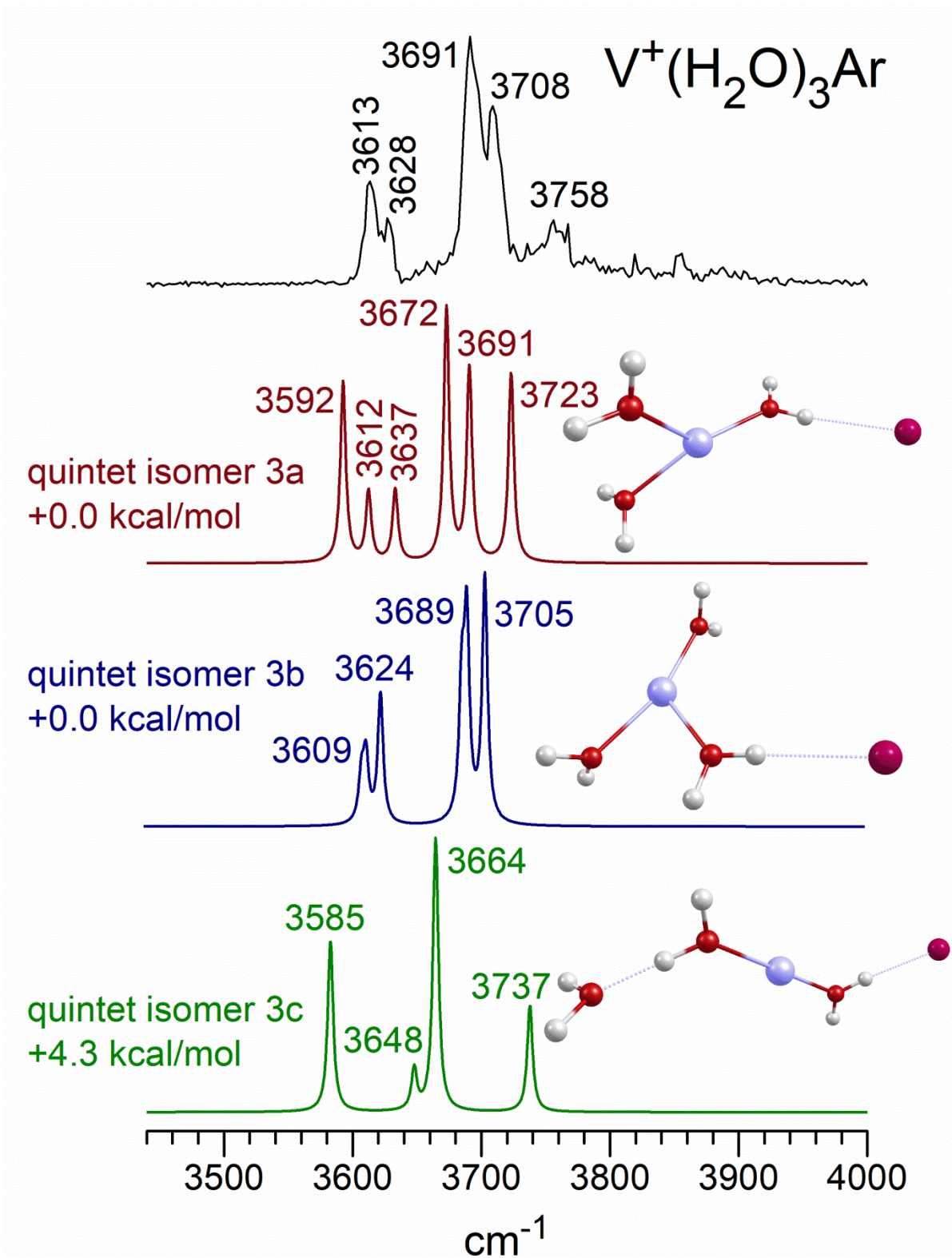


Figure 6.

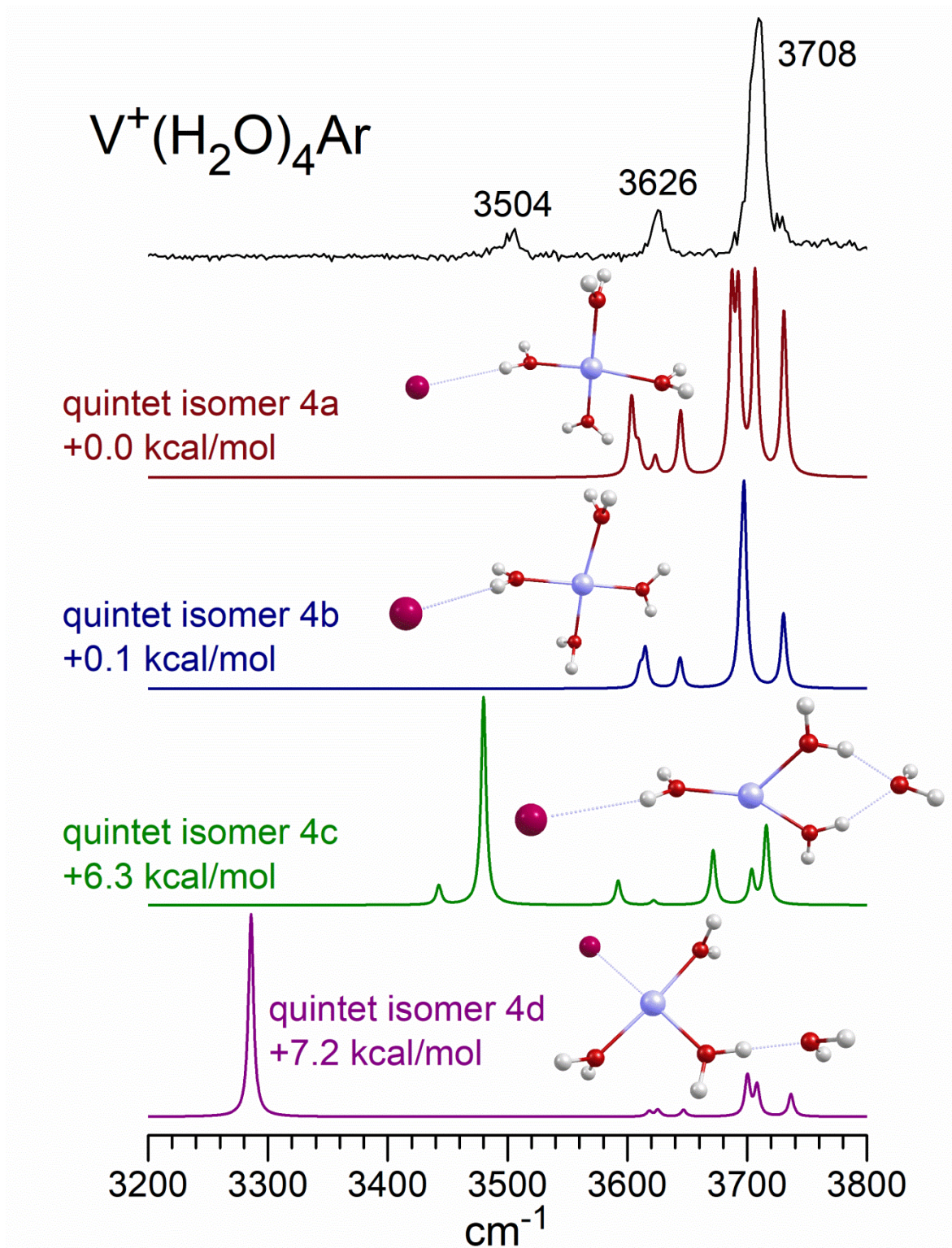


Figure 7.

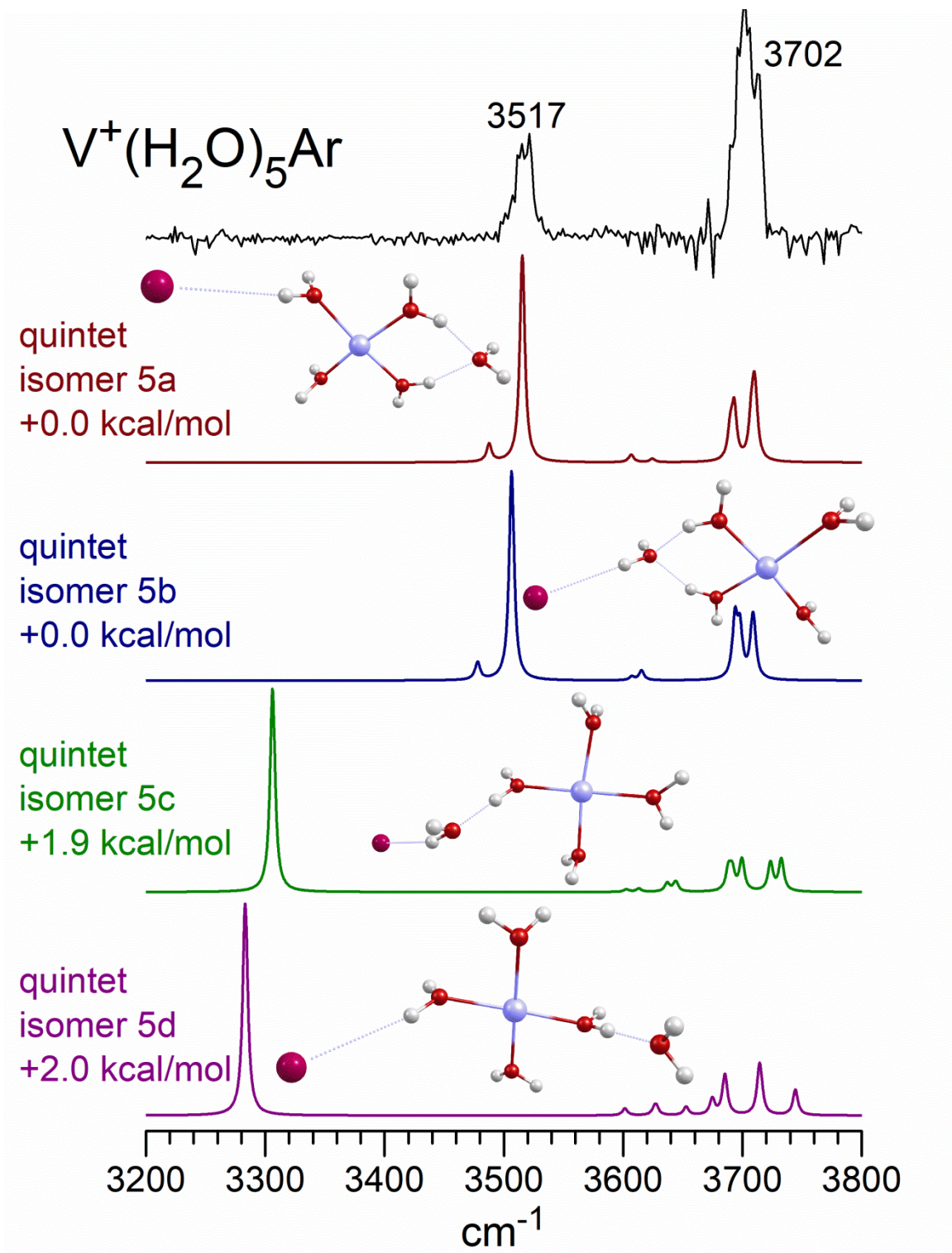


Figure 8.

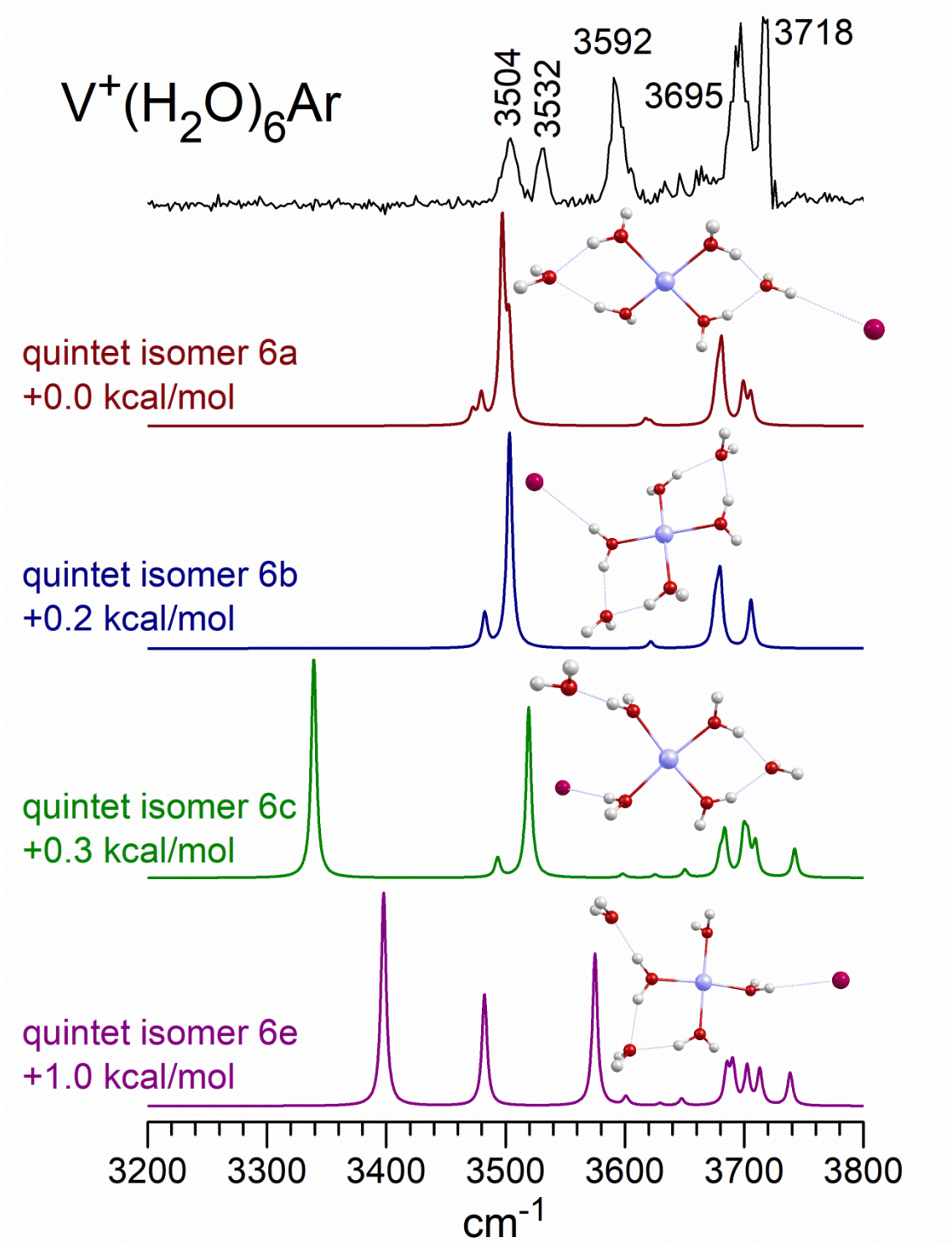


Figure 9.

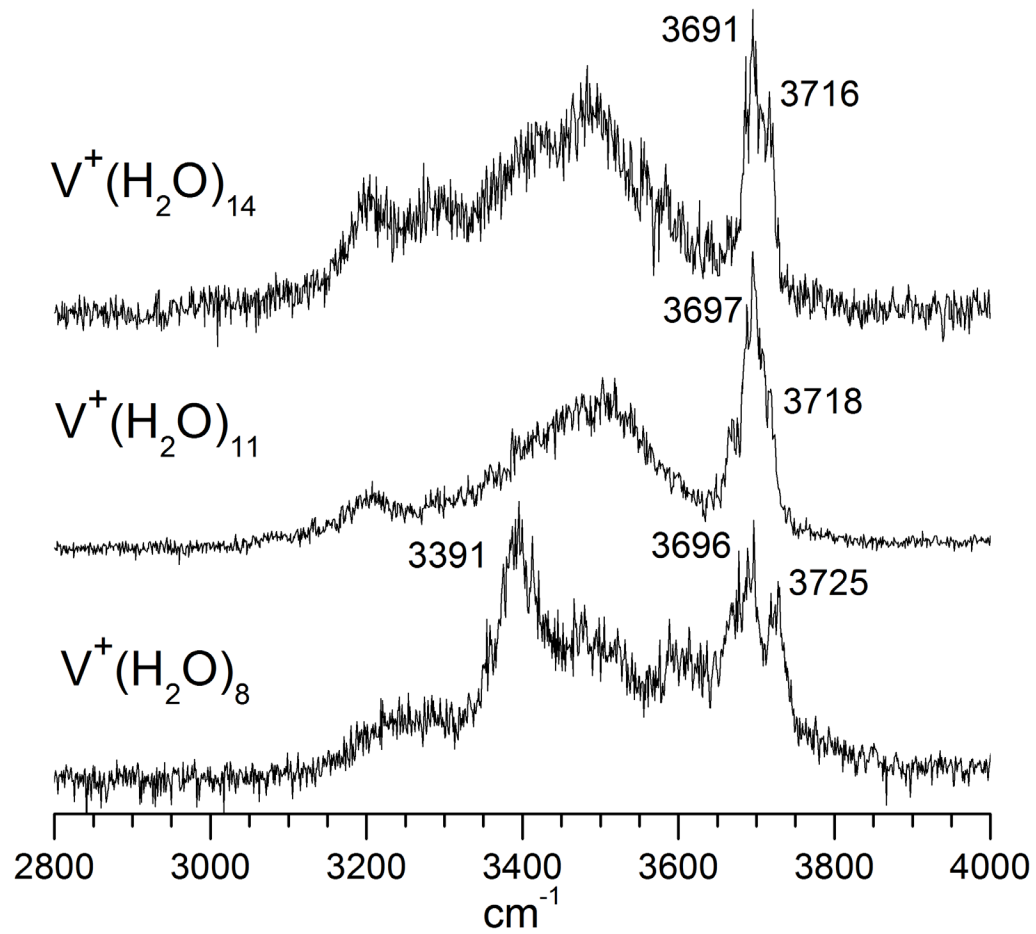


Figure 10.

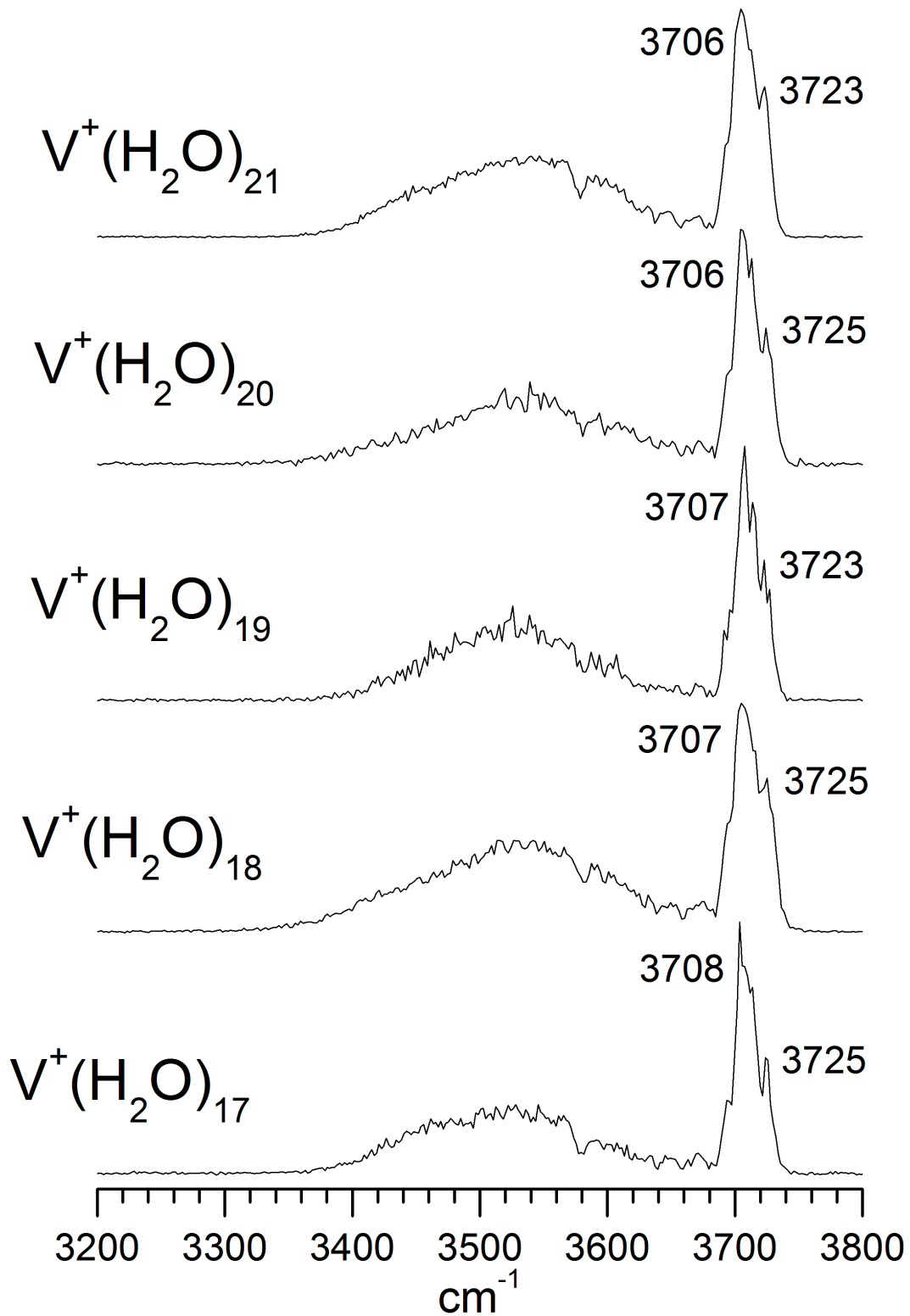


Figure 11.

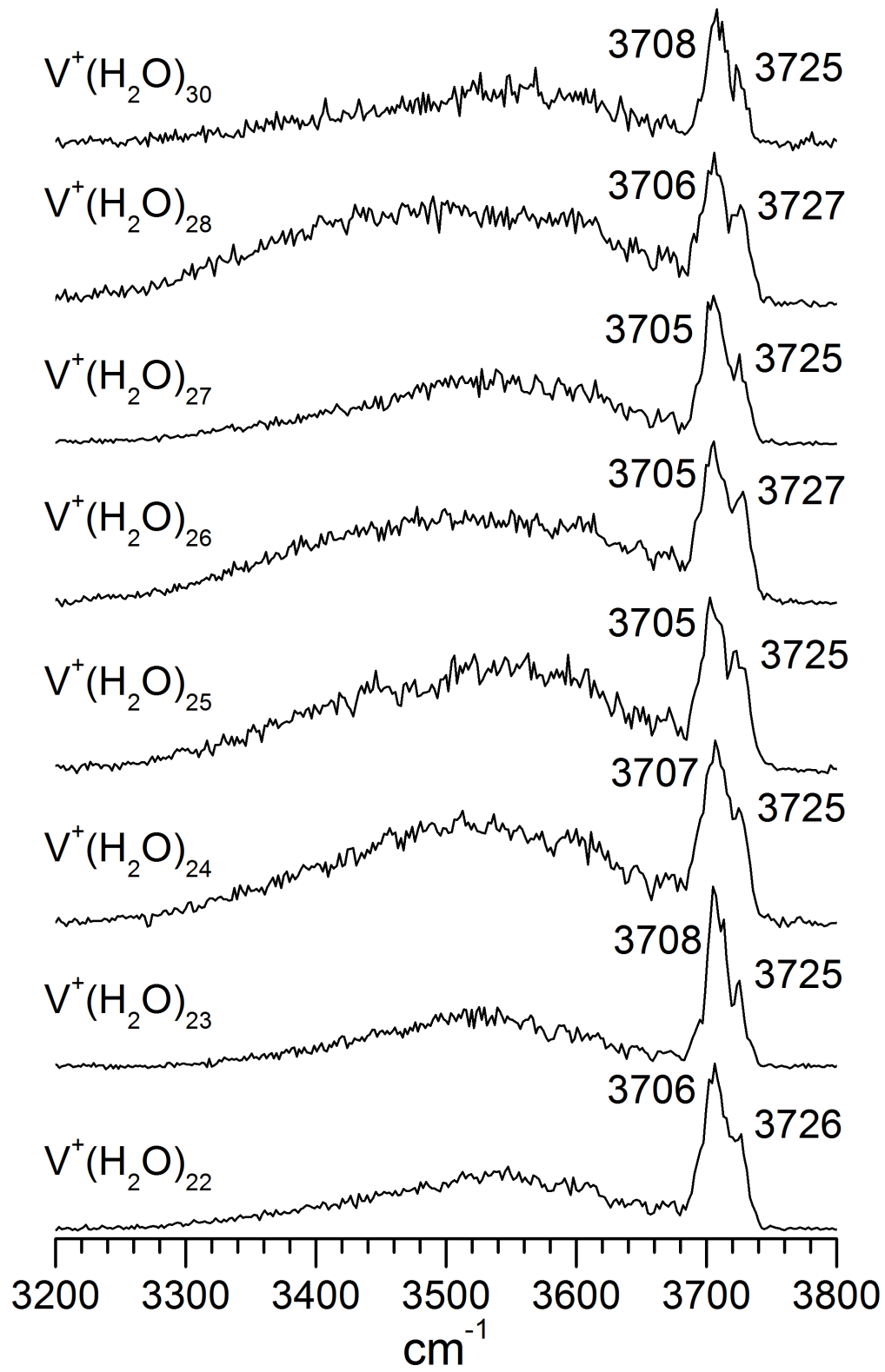


Figure 12.

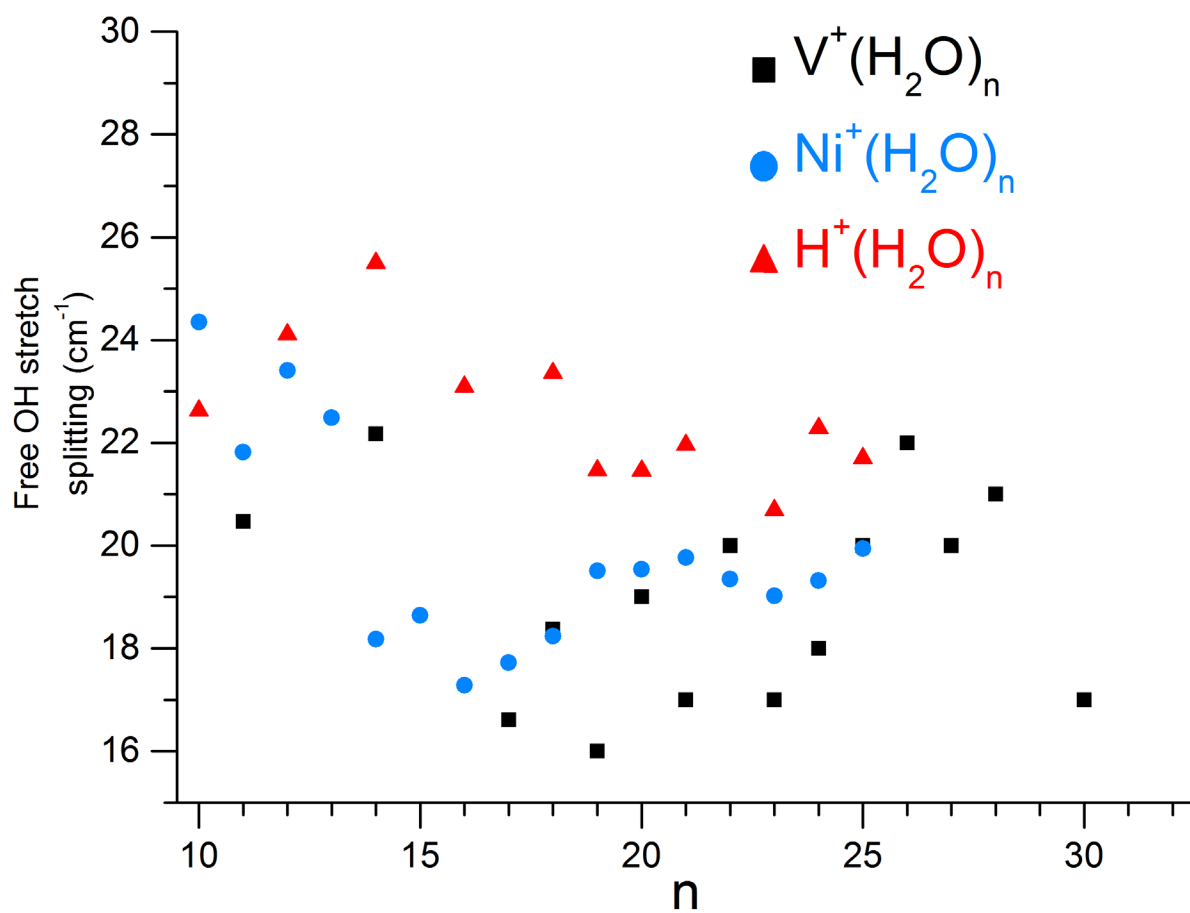


Figure 13.

TOC Graphic:

